Available online at www.sciencedirect.com
SCIENCE DIRECT®
Applied Geochemistry 19 (2004) 1905–1926
Applied Geochemistry
www.elsevier.com/locate/apgeochem

# The evolution of alkaline, saline ground- and surface waters in the southern Siberian steppes

D. Banks[a,*], V.P. Parnachev[b], B. Frengstad[c], W. Holden[d], O.V. Karnachuk[e], A.A. Vedernikov[f]

[a]Holymoor Consultancy, 8 Heaton Street, Brampton, Chesterfield, Derbyshire S40 3AQ, UK
[b]Department of Dynamic Geology, Tomsk State University, Prospekt Lenina 36, 634050 Tomsk, Russia
[c]Norges Geologiske Undersøkelse, N7491 Trondheim, Norway
[d]URS Dames & Moore, St. George's House (2nd Floor), 5 St. George's Road, Wimbledon, London SW19 4DR, UK
[e]Department of Agriculture and Environmental Science, Tomsk State University, Prospekt Lenina 36, 634050 Tomsk, Russia
[f]State Committee for Environmental Protection of the Republic of Khakassia, Abakan, Republic of Khakassia, Russia

Received 25 November 2002; accepted 26 May 2004

Editorial handling by C. Reimann

**Abstract**

Groundwaters, river and lake waters have been sampled from the semi-arid Siberian Republic of Khakassia. Despite the relatively sparse data set, from a diversity of hydrological environments, clear salinity-related trends emerge that indicate the main hydrochemical evolutionary processes active in the region. Furthermore, the major ion chemistry of the evolution of groundwater baseflow, via rivers, to terminal saline lake water, can be adequately and simply modelled (using PHREEQCI) by invoking: (i) degassing of $CO_2$ from groundwater as it emerges as baseflow in rivers (rise in pH); (ii) progressive evapoconcentration of waters (parallel accumulation of $Cl^-$, $Na^+$, $SO_4^{2-}$, and increase in pH due to common ion effect); and (iii) precipitation of calcite (depletion of Ca from waters, reduced rate of accumulation of alkalinity). Dolomite precipitation is ineffective at constraining Mg accumulation, due to kinetic factors. Silica saturation appears to control dissolved Si in low salinity waters and groundwaters, while sepiolite saturation and precipitation depletes Si from the more saline surface waters. Gypsum and sodium sulphate saturation are only approached in the most saline environments. Halite remains unsaturated in all waters. Sulphate reduction processes are important in the lower part of lakes.


## 1. Introduction and objectives

During the period 1996–2000, a program of sampling and analysis of groundwaters, river and lake waters was carried out in the southern Siberian Republic of Khakassia (part of the Russian Federation) by Tomsk State University, for the Khakassian State Committee for Environmental Protection. The main objective of the overall study was to document and characterise the "baseline" natural hydrochemistry of the Republic. The study has resulted in the production of hydrochemical monographs and scientific articles, including those by Parnachev et al. (1997, 1999a,b, 2003), Banks et al. (1998, 2001), Makarenko et al. (1999) and Parnachev and Degermendzhy (2002).

The steppes of southern Russia and Siberia represent a huge, relatively coherent, climatic, hydrological and geochemical environment, the evolution of whose waters

* Corresponding author. Tel.: +44-1246-230068; fax: +44-1246-230068.
*E-mail address:* david@holymoor.co.uk (D. Banks).

0883-2927/$ - see front matter © 2004 Elsevier Ltd. All rights reserved.
doi:10.1016/j.apgeochem.2004.05.009

is not well documented or understood, especially in western literature. Furthermore, the steppe environment shares some common features (e.g., a tendency to water and soil salinization, evolution of Na–Cl–$SO_4$ waters, terminal high pH saline lakes and deposition of evaporites) with other seasonally cold, semi-arid, hydrologically "closed" environments, occupying significant areas of the earth's surface, such as the Canadian prairies and the Bolivian Altiplano. These areas are characterised by commercially important evaporite sequences, containing reserves of, e.g., $Na_2SO_4$, B and Li (Harben and Kuzvart, 1996; Troëng and Riera-Kilibarda, 1996).

This particular paper focuses on two data sets resulting from sampling rounds in 1999 and 2000, dominantly in the central part of Khakassia, and analysed at the Geological Survey of Norway. The objective of the paper is to ascertain whether such data sets really can reveal important hydrochemical evolutionary processes in ground- and surface waters, despite the fact that they:

(a) are geographically sparse (only some 60 samples in an area of some 20,000 $km^2$),
(b) do not derive from systematically chosen sample locations (given that sampling locations were constrained by the relatively low density of groundwater abstractions and surface water features),
(c) contain data from varied geological, topographical and hydrological environments.

This paper argues in the affirmative: even a relatively sparse data set, containing samples from a wide variety of hydrological media, has considerable utility. Furthermore, this paper attempts to demonstrate, by applying relatively simple hydrochemical modelling techniques to the data set, that a limited number of geochemical processes coupled with evaporative concentration can explain many of the major ion hydrochemical features of the area, including the evolution of groundwater baseflow, via river water, to the water quality observed in terminal saline lakes in the area.

## 2. The study area

The Republic of Khakassia is located in southern central Siberia, within the region of the Altai-Sayan Mountains (Fig. 1). The western margins of the Republic comprise the Kuznetsk Alatau Mountains (rising to a maximum altitude of 2178 m asl), while the southern fringes are dominated by the Western Sayan (maximum 2930 m). A large part of the eastern border is formed by the River Yenisei. The other major watercourse of the Republic is the River Abakan, rising in the mountainous SW and flowing through Abaza and Askiz to its confluence with the Yenisei near Abakan city.

The climate of Khakassia is highly continental and becomes more extreme towards the lowlands of the east (Fig. 2, Balakhchina et al., 1999). Fig. 3 shows typical precipitation and temperature data for Abakan, which enjoys less than 400 mm precipitation per year. Winter temperature minima can fall to −50 °C while summer maxima rise to +36 °C. At Lake Shira (at 352 m asl; see Fig. 1), open water evaporation is reported to be around 600 mm/a (http://www.lan.krasu.ru/rec/collect%5Cshira_e.html). Further west, into the mountains, the temperature range becomes somewhat less extreme and up to 1500 mm precipitation are recorded annually in the mountains of the extreme SW. Khakassia does not experience regional permafrost conditions.

The upland areas (Sayan, Kuznetsk Alatau mountains) are characterised by erosionally resistant Precambrian and Lower Palaeozoic metasedimentary, metavolcanic and plutonic rocks. They are often wooded by taiga-like vegetation and exhibit freshwater lakes and fresh groundwaters.

The lowland areas in the centre-east of the Republic (Shira, Askiz-Abakan) are characterised by low rainfall, extreme temperature ranges, a tendency towards salinization of soils and groundwaters (Balakhchina et al., 1999), steppe landscape and the presence of both fresh and saline lakes. Limited agriculture takes place in these areas, although much of the steppe landscape is subject to cattle ranching. Soil types reflect topography, with mountainous taiga landscape typically being underlain by (using the Russian terminology – see Stolbovoi, 1998) weakly acidic to acidic grey forest *greyzems*, *podzolics* and brown forest soils. In the foothills, mountain *chernozems* (black soils), grey mountain forest greyzems and forest-sod soils dominate. Moving into the steppe area, leached, southern and ordinary *chernozems* occur, with dark haplic *kastanozems* in the dryer parts. In specific areas of the steppes, dark alkaline soils (*solonets*) and saline soils (*solonchak*) prevail (Balakhchina et al., 1999).

The lowland areas represent an early Devonian palaeo-rift structure, termed the Minusinsk Depression (Luchitsky, 1960; Parnachev et al., 1992), comprising several sub-basins and infilled by a variety of sedimentary and volcano-sedimentary rocks of Lower Devonian to Permian age (Fig. 4). The lithologies present vary slightly from sub-basin to sub-basin but are described by Parnachev et al. (1999b) and Banks et al. (2001). They are broadly speaking proximal sediments of red-bed molasse type and contain gypsum-bearing interbeds. The Lower Devonian and Lower Carboniferous formations are particularly distinguished by volcanics and tuffs, while carbonates are characteristic of the Middle Devonian and "Old-Red" facies of the Upper Devonian. Economically exploitable coals occur within the Carboniferous and Permian, especially around Abakan (Banks et al., 2002b).

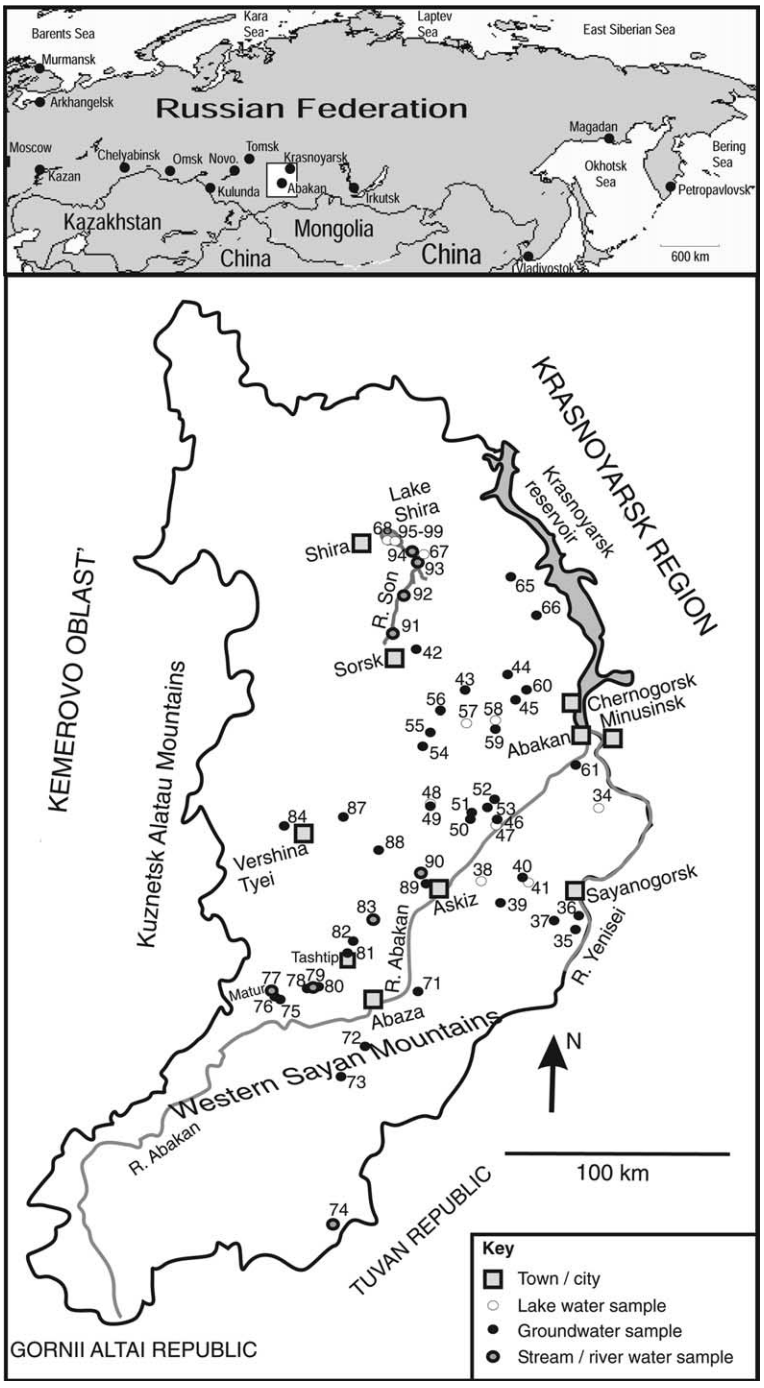


Fig. 1. Outline map of the Republic of Khakassia, showing locations of sampling points. Locations named in text: Lake Kurinka = no. 34; Lake Utinoe = no. 38; Lake Chernoe = no. 41; Lake Solenoe = no. 47; Lake Bulankul = no. 48; Lake Ulugkol = no. 57; Lake Uskol = no. 58; Moskovskii Sovkhoz = no. 60; Polindeika = no. 66; Lake Vlasyevo = no. 67. Upper map shows location of Khakassia within the Russian Federation: Novo. = Novosibirsk.

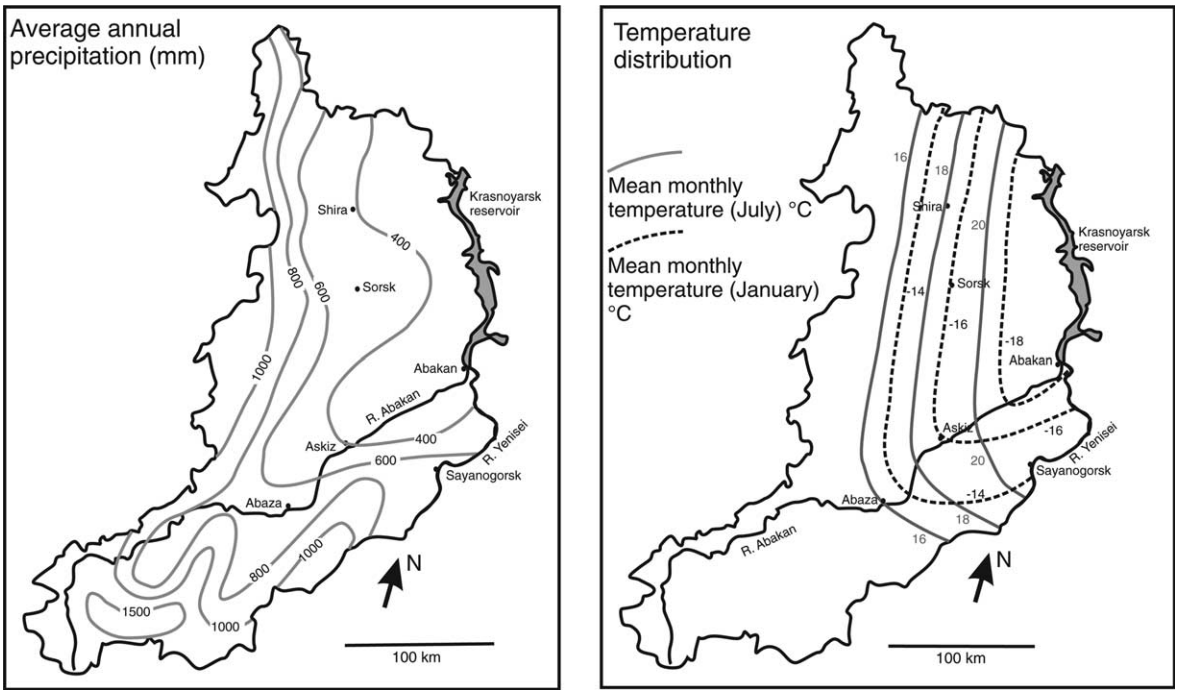


Fig. 2. Outline maps of Khakassia, showing contours on (left) annual average precipitation (mm), and (right) mean monthly temperatures for January and July (°C), modified after Balakhchina et al. (1999).

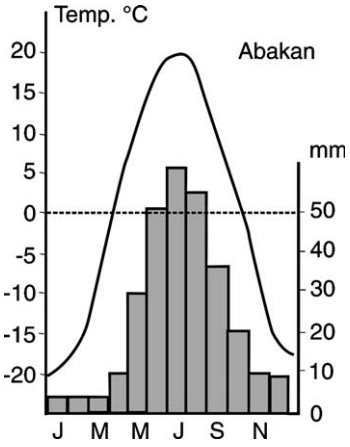


Fig. 3. Average seasonal variation in temperature and precipitation at Abakan, modified after Balakhchina et al. (1999).

## 3. Previous hydrochemical studies of Khakassia

The saline lakes of lowland Khakassia have long been regarded as having potential as spa resorts and have been the subject of studies by Russian scientists as far back as the investigations of Lake Shira by E. Meller in 1876. Subsequent descriptions of Shira, Shunyet and other lakes are published by Savenkov (1890), Predtechensky (1912), Orlov (1921) and the renowned Kurlov (1927, 1928, 1929). Parnachev and Degermendzhy (2002) provide a concise summary of the broad hydrochemical attributes of Khakassia's saline lakes, while papers, including those by Kalacheva et al. (2002) and Gaevsky et al. (2002), appear in a thematic volume (Aquatic Ecology, vol. 36, No. 2) on the ecology of Lake Shira. Banks (1998) compared the hydrochemistry of granitic aquifers in Khakassia with those of Norway and Great Britain. Banks et al. (2002a) discussed probable bacterial and N contamination of Khakassian groundwater by pit latrines and other contamination sources in towns and villages. A further paper by Banks et al. (2002b) considered the composition of mine waters from coal and metals mines in Khakassia.

A limited study, in August 1996, of groundwaters in the Shira Region of Khakassia aimed to shed light on the evolution of groundwater chemistry. The main conclusions (Banks et al., 1998; Parnachev et al., 1999b) of that study were as follows:

- The region exhibits many characteristics common to other cold, semi-arid areas of the world: a continental climate, location in a rain shadow, low density of surface water drainage, occurrence of palaeo- and modern evaporite mineralization, occurrence of saline lakes and saline groundwaters, often of Na–$SO_4$–Cl composition.
- The evolution of Na–$SO_4$–Cl groundwaters can be explained by a combination of silicate weathering,

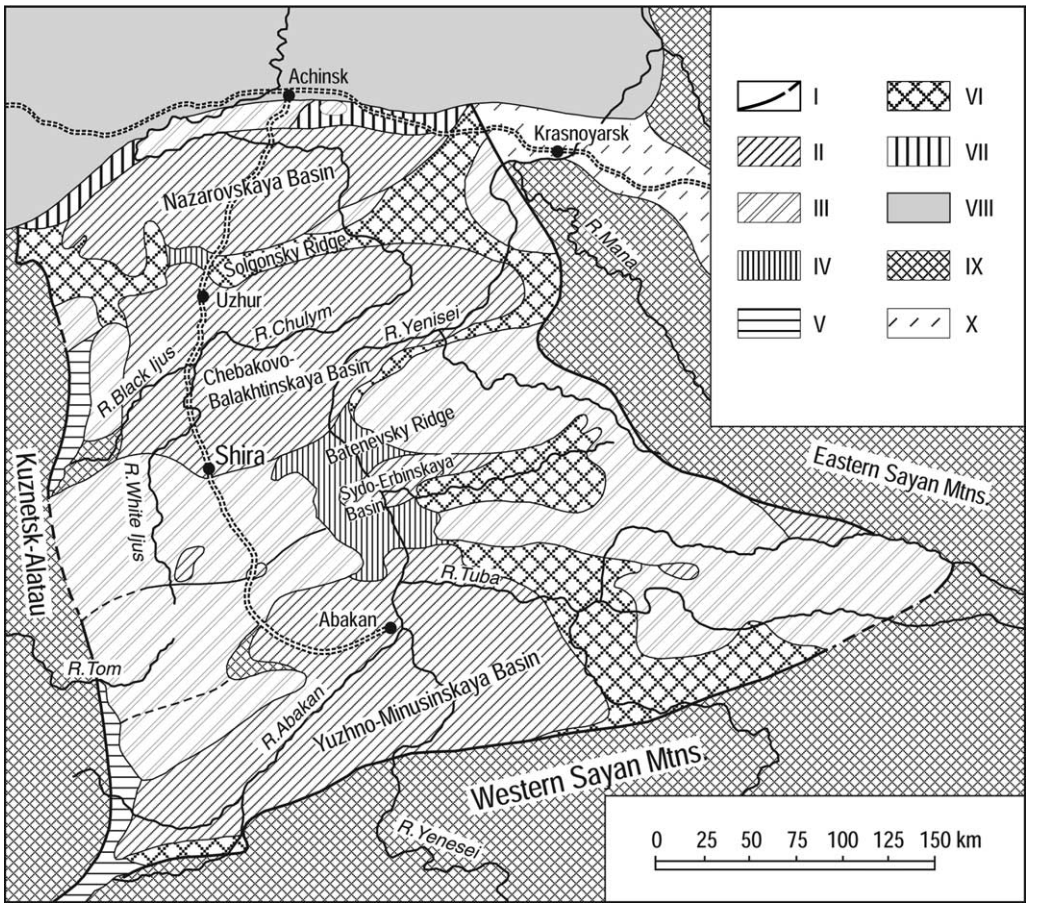


Fig. 4. Sketch map of the Minusinsk intermontane trough within the Altai-Sayan mountain region, Khakassia, southern Siberia, Russia (after Luchitsky, 1960). Key: I – boundary of the Minusinsk trough; II – the main Devonian sub-basins; III – Horst/ridge areas between sub-basins; IV,V – depressions; VI – horst/ridge area, beneath cover of Devonian volcanogenic rocks; VII – ditto, beneath cover of Mesozoic (mainly Jurassic) deposits; VIII – Chulimskaya synclinorium (Mesozoic sediments); IX – Pre-Devonian magmatic and metamorphic formations surrounding the Minusinsk trough (i.e., basement); X – basement, beneath cover of mid-Palaeozoic sedimentary rocks. See Fig. 1 for location.

gypsum and halite dissolution (both of which occur in the Devonian sequence as palaeo-evaporite minerals), coupled with calcite precipitation and some degree of evaporative concentration.

- Na–$SO_4$–Cl signatures in saline soils and waters are redistributed throughout the project area by precipitation and atmospheric transport of dust.

The hydrochemical evolution of Khakassia surface waters and the relationship between surface and groundwaters remain poorly studied, however. It is these aspects that the current paper attempts to address.

## 4. Sampling and analytical techniques

The data sets, comprising 36 groundwater samples, 9 river water samples (from 6 rivers) and 14 lake water samples (from 9 lakes), upon which the current study is based, were collected during two periods of fieldwork and sampling. First during June 1999, samples Xa34–Xa68 (Fig. 1) were taken of lake waters and groundwaters (wells, boreholes and springs), mostly in the Abakan area. Samples were also taken of modern evaporite crusts around lakes and in spring areas for analysis by X-ray diffraction (XRD). Secondly, during September 2000, samples Xa70–Xa94 were taken of groundwater and river/stream water in the vicinity of Abaza, Askiz, Sonskii (Fig. 7), Shira and Vershina Tyei. In addition, depth sampling and hydrochemical profiling were carried out from a boat in Lake Shira (Xa95–99).

Detailed descriptions of sample locations and analytical procedures are provided in Banks et al. (2001). However, to summarize: groundwater samples were taken, to the extent possible, from flowing sources (springs

Table 1
Main hydrochemical characteristics of sampled groundwaters and surface waters

| No. | Location | Geol-ogy | Type | Depth (m) | $H_2S$ | pH | $T$ (°C) | Alk (meq/L) | Eh (mV) | $F^-$ (mg/L) | $Cl^-$ (mg/L) | $NO_3^-$ (mg/L) | $SO_4^{2-}$ (mg/L) | Si (mg/L) | Mg (mg/L) | Ca (mg/L) | Na (mg/L) | K (mg/L) | B (mg/L) | Water type | Alk/Ca (meq/L) |
|---|---|---|---|---|---|---|---|---|---|---|---|---|---|---|---|---|---|---|---|---|---|
| *Groundwaters* | | | | | | | | | | | | | | | | | | | | | |
| 35 | Marble quarry | R1, R2 | 1 | 60 | 0 | 7.52 | 7.5 | 3.7 | [+77] | 0.05 | 34.4 | 6.4 | 5.29 | 8.23 | 5.66 | 80.7 | 3.59 | 2.47 | <0.02 | $Ca–HCO_3–Cl$ | 0.92 |
| 36 | Maina | K1 | 1 | 35 | 0 | 7.55 | 8.0 | 3.8 | [+40] | 0.18 | 0.69 | 4.5 | 8.30 | 5.14 | 8.38 | 60.2 | 5.41 | <0.5 | <0.02 | $Ca–HCO_3$ | 1.26 |
| 37 | Bogoslovka | K1/Q? | 1 | 45 | 0 | 7.61 | 6.1 | 5.1 | [+150] | 0.25 | 2.17 | 8.9 | 5.61 | 6.91 | 29.4 | 52.7 | 5.88 | 0.89 | 0.022 | $Ca–Mg–HCO_3$ | 1.94 |
| 39 | Byeya Dairy | D2 | 1 | 40 | 0 | 7.30 | 6.8 | 4.7 | 205 | <0.05 | 7.05 | 10.1 | 21.9 | 6.05 | 11.0 | 82.2 | 7.24 | 0.81 | <0.02 | $Ca–HCO_3$ | 1.15 |
| 40 | Novotroitskaya | D3 | 1 | ? | 1 | 8.09 | 6.1 | 10.9 | [+155] | 1.60 | 192 | 212 | 578 | 2.61 | 20.3 | 19.1 | 662 | 2.33 | 1.06 | $Na–SO_4–HCO_3$ | 11.44 |
| 42 | Tumannii | K2 | 2 | ? | 0 | 7.79 | 2.9 | 4.5 | 180 | 0.98 | 1.95 | 1.5 | 14.5 | 7.58 | 21.2 | 47.6 | 16.0 | 1.03 | <0.02 | $Ca–Mg–HCO_3$ | 1.89 |
| 43 | Mount Amoga Spring | R3 | 3 | ? | 0 | 7.35 | 9.6 | 6.2 | 210 | 0.61 | 5.13 | 4.9 | 63.0 | 3.71 | 35.2 | 75.7 | 15.7 | 1.46 | <0.02 | $Ca–Mg–HCO_3$ | 1.64 |
| 44 | Vershino Bidzha Spring | R3 | 3 | ? | 0 | 7.39 | 7.8 | 5.6 | 215 | 0.66 | 4.48 | 4.3 | 49.7 | 3.96 | 33.3 | 68.6 | 15.2 | 1.37 | 0.031 | $Ca–Mg–HCO_3$ | 1.64 |
| 45 | SW of Moscov-skii | C1 | 3 | ? | 1 | 8.35 | 11.5 | 10.8 | <+100 | 1.43 | 747 | 5.3 | 1939 | 3.80 | 65.1 | 95.3 | 1320 | 3.84 | 2.49 | $Na–SO_4–Cl$ | 2.27 |
| 46 | Khan Kul borehole | D3 | 2 | 350 ? | 0 | 8.04 | 6.2 | 6.8 | <+100 | 0.95 | 84.9 | 24.6 | 1418 | 3.22 | 82.0 | 87.7 | 553 | 3.59 | 1.31 | $Na–SO_4$ | 1.55 |
| 49 | Sanatorium Bulankul | K–O | 1 | 45 | 0 | 7.41 | 3.9 | 6.5 | [+145] | 0.89 | 8.39 | 15.0 | 11.9 | 7.00 | 30.6 | 59.8 | 25.9 | 2.43 | 0.040 | $Ca–Mg–HCO_3$ | 2.18 |
| 50 | E of Pulankul | D1 | 1 | 25 ? | 0 | 7.49 | 6.1 | 4.4 | [+78] | 0.79 | 7.75 | 7.3 | 46.0 | 6.44 | 13.8 | 69.7 | 18.3 | 1.18 | 0.038 | $Ca–Mg–HCO_3$ | 1.27 |
| 51 | Vtoroi Kluch | K(–O) | 3 | ? | 0 | 7.34 | 4.8 | 4.5 | 142 | 0.99 | 14.3 | 20.2 | 41.5 | 5.98 | 21.3 | 63.6 | 27.9 | 1.57 | 0.035 | $Ca–Mg–HCO_3$ | 1.42 |
| 52 | Mount Timirtag | D2 | 2 | ? | – | 7.50 | 6.0 | 4.1 | −14 | 0.69 | 6.27 | 6.5 | 154 | 4.40 | 21.1 | 93.2 | 19.4 | 1.89 | 0.089 | $Ca–Mg–HCO_3–SO_4$ | 0.88 |
| 53 | Kharasug Spring | D2 (K–O) | 3 | ? | 0 | 7.48 | 4.5 | 3.9 | 177 | 0.81 | 7.43 | 9.3 | 41.4 | 5.24 | 10.2 | 67.6 | 13.5 | 1.58 | 0.051 | $Ca–HCO_3$ | 1.16 |
| 54 | Charkov | D2/D3/?Q? | 1 | ? | 0 | 7.51 | 6.3 | 5.2 | 68 | 0.94 | 16.7 | 6.2 | 73.8 | 5.28 | 33.1 | 63.8 | 32.1 | 2.82 | 0.044 | $Ca–Mg–HCO_3–SO_4$ | 1.63 |
| 55 | N of Charkov | D1 | 3 | ? | 0 | 7.64 | 7.0 | 6.3 | 139 | 0.42 | 24.2 | 11.3 | 90.0 | 5.65 | 31.8 | 74.5 | 46.4 | 2.83 | 0.042 | $Ca–Mg–Na–HCO_3–SO_4$ | 1.69 |
| 56 | Ust Kamisyak | C1 | 3 | ? | 0 | 7.38 | 7.3 | 6.5 | 190 | 0.50 | 3.83 | 5.3 | 40.2 | 3.82 | 28.7 | 64.6 | 26.9 | 1.21 | 0.024 | $Ca–Mg–HCO_3$ | 2.02 |
| 59 | Abakanskii 2 saltwell | D3 | 5 | ? | 1 | 7.41 | 10.6 | 5.9 | [<+100] | (300) | 56325 | <50 | 8372 | 1.63 | 1990 | 963 | 31700 | 83.2 | 1.58 | Na–Cl | 0.12 |
| 60 | Moskovskii Sov-khoz | D2 | 1 | ? | 0 | 7.27 | 4.8 | 7.0 | [+110] | 0.60 | 124 | 87.2 | 456 | 5.55 | 92.1 | 120 | 143 | 2.28 | 0.17 | $Mg–Na–Ca–SO_4–HCO_3$ | 1.17 |
| 61 | Byelii yar mine borehole | Q | 1 | 32 | 0 | 7.92 | 10.1 | 4.1 | [+130] | 0.58 | 54.3 | 15.2 | 88.5 | 6.27 | 27.8 | 49.1 | 67.5 | 1.68 | 0.038 | $Na–Ca–Mg–HCO_3–SO_4$ | 1.67 |
| 65 | Znamenka | D2 | 1 | ? | 0 | 7.59 | 5.0 | 6.7 | [+127] | 0.66 | 96.8 | 28.7 | 331 | 6.16 | 80.4 | 126 | 79.7 | 3.12 | 0.093 | $Mg–Ca–Na–SO_4–HCO_3$ | 1.07 |
| 66 | Polindeika | D1 | 1 | ? | 0 | 8.13 | 7.3 | 2.9 | [+50] | 0.65 | 128 | 10.0 | 143 | 4.93 | 13.1 | 53.1 | 133 | <0.5 | 0.035 | $Na–Ca–Cl–SO_4–HCO_3$ | 1.09 |
| 71 | Silver Spring II | LPS | 3 | 0 | 0 | 7.33 | 8.3 | 2.8 | – | 0.18 | 6.88 | 0.71 | 6.27 | 6.67 | 11.5 | 45.4 | 13.7 | 0.96 | <0.02 | $Ca–Mg–HCO_3$ | 1.23 |
| 72 | km 212 | LPS | 3 | 0 | 0 | 8.10 | 7.5 | 3.4 | – | 0.09 | 1.12 | 1.4 | 11.2 | 5.38 | 13.1 | 77.0 | 4.13 | 1.51 | <0.02 | $Ca–Mg–HCO_3$ | 0.88 |
| 73 | Radon spring km 223 | LPS | 3 | 0 | 0 | 7.76 | 4.1 | 2.5 | – | 0.07 | 0.55 | 2.1 | 5.98 | 4.30 | 8.06 | 60.8 | 2.82 | 0.84 | <0.02 | $Ca–Mg–HCO_3$ | 0.81 |
| 75 | Matur borehole | D12 | 1 | 90 | 0 | 7.55 | 5.8 | 4.3 | – | 0.14 | 2.8 | 13.0 | 8.24 | 5.55 | 18.5 | 101 | 6.40 | 0.82 | <0.02 | $Ca–Mg–HCO_3$ | 0.86 |

| | | | | | | | | | | | | | | | | | | | | |
|---|---|---|---|---|---|---|---|---|---|---|---|---|---|---|---|---|---|---|---|---|
| 76 | Matur private well | Q | 5 | 6 | 0 | 7.28 | 7.5 | 6.3 | – | 0.10 | 75.1 | 39.6 | 150 | 6.44 | 30.8 | 232 | 40.1 | 1.93 | <0.02 | $Ca–HCO_3–SO_4$ | 0.55 |
| 78 | Baza DRSU Shepchul | D12 | 1 | 35 | 0 | 7.33 | 6.0 | 5.4 | – | 0.25 | 0.32 | 1.7 | 7.97 | 5.52 | 17.0 | 127 | 7.11 | 0.97 | 0.020 | $Ca–Mg–HCO_3$ | 0.86 |
| 80 | Verkhnaya Syeya | D12 | 1 | 30 | 0 | 7.52 | 7.5 | 4.8 | – | 0.14 | 5.64 | 7.9 | 25.0 | 6.54 | 19.4 | 114 | 7.37 | 1.07 | <0.02 | $Ca–Mg–HCO_3$ | 0.85 |
| 81 | Tashtip North | D12 | 1 | 40 | 0 | 7.45 | 9.8 | 5.5 | – | 0.36 | 3.77 | 9.9 | 36.9 | 6.43 | 29.6 | 108 | 37.7 | 1.43 | 0.034 | $Ca–Mg–Na–HCO_3$ | 1.01 |
| 82 | Imek North | D12 | 1 | 100 | 0 | 7.37 | 14.5 | 5.2 | – | 0.30 | 28.0 | 23.6 | 256 | 5.73 | 42.3 | 150 | 67.2 | 2.03 | 0.061 | $Ca–Mg–Na–SO_4–HCO_3$ | 0.69 |
| 84 | Vershina Tyei bore | LPS | 1 | 35 | 0 | 7.93 | 4.9 | 2.4 | – | <0.05 | 0.47 | 2.2 | 6.97 | 4.32 | 10.5 | 48.8 | 1.90 | 0.62 | <0.02 | $Ca–Mg–HCO_3$ | 0.99 |
| 87 | Silver spring Birikchul | C–O | 3 | 0 | 0 | 7.75 | 4.5 | 2.8 | – | 0.30 | 1.1 | 3.6 | 20.6 | 6.94 | 9.94 | 62.8 | 6.46 | 0.67 | <0.02 | $Ca–Mg–HCO_3$ | 0.91 |
| 88 | Kazanovka station | D12 | 1 | 75 | 0 | 7.44 | 9.9 | 3.3 | – | 0.25 | 93.1 | 27.8 | 618 | 5.65 | 77.1 | 201 | 69.5 | 4.54 | 0.073 | $Ca–Mg–SO_4$ | 0.32 |
| 89 | Askiz station | D3 | 1 | 40 | 0 | 7.53 | 4.0 | 4.8 | – | 0.33 | 75.8 | 26.0 | 199 | 5.27 | 43.3 | 116 | 102 | 3.99 | 0.14 | $Ca–Na–Mg–HCO_3–SO_4$ | 0.84 |
| *Stream waters* | | | | | | | | | | | | | | | | | | | | | |
| 74 | River Bolshoi On | | 7 | 0 | 0 | 8.00 | 6.1 | 0.6 | – | <0.05 | 0.15 | 0.96 | 1.70 | 2.01 | 1.34 | 10.3 | 0.933 | <0.5 | <0.02 | $Ca–HCO_3$ | 1.19 |
| 77 | River Matur | D12 | 7 | 0 | 0 | 8.38 | 11.4 | 4.4 | – | 0.12 | 0.84 | 0.8 | 37.8 | 5.78 | 18.5 | 101 | 7.54 | 0.71 | <0.02 | $Ca–Mg–HCO_3$ | 0.88 |
| 79 | River Bolshaya Syeya | D12 | 7 | 0 | 0 | 8.48 | 13.1 | 3.8 | – | 0.09 | 1.03 | <0.05 | 24.8 | 4.22 | 10.5 | 74.6 | 5.64 | 1.00 | <0.02 | $Ca–HCO_3$ | 1.01 |
| 83 | River Tyeya | D3 | 7 | 0 | 0 | 8.80 | 15.7 | 2.5 | – | 0.11 | 4.43 | 1.2 | 36.4 | 3.29 | 9.16 | 48.3 | 5.82 | 1.00 | <0.02 | $Ca–Mg–HCO_3–SO_4$ | 1.06 |
| 90 | River Baza | D3 | 7 | 0 | 0 | 8.47 | 7.0 | 4.2 | – | 0.26 | 2.48 | 2.1 | 18.0 | 3.87 | 20.1 | 69.6 | 7.36 | 1.36 | <0.02 | $Ca–Mg–HCO_3$ | 1.22 |
| 91 | River Son Sonskii | LPV | 7 | 0 | 0 | 8.25 | 7.2 | 3.7 | – | 0.37 | 0.53 | <0.05 | 20.0 | 5.69 | 11.3 | 59.0 | 3.86 | 0.81 | <0.02 | $Ca–Mg–HCO_3$ | 1.26 |
| 92 | River Son Katjushkino | | 7 | 0 | 0 | 8.54 | 6.8 | 5.1 | – | 0.43 | 5.11 | 3.4 | 33.3 | 5.36 | 22.1 | 81.7 | 7.26 | 1.66 | <0.02 | $Ca–Mg–HCO_3$ | 1.25 |
| 93 | River Son S of Borets | D2 | 7 | 0 | 0 | 8.33 | 6.3 | 6.9 | – | 0.70 | 8.66 | 0.60 | 68.0 | 6.79 | 33.2 | 82.1 | 31.6 | 1.79 | 0.034 | $Ca–Mg–HCO_3$ | 1.68 |
| 94 | River Son ds Borets | D2 | 7 | 0 | 0 | 8.64 | 4.8 | 7.2 | – | 0.69 | 14.5 | 0.34 | 98.0 | 6.11 | 39.8 | 85.4 | 42.2 | 1.73 | 0.057 | $Ca–Mg–HCO_3–SO_4$ | 1.68 |
| *Lake waters* | | | | | | | | | | | | | | | | | | | | | |
| 34 | Lake Kurinka | D3, C1 | 4 | – | 2 | 10.11 | 20.0 | 35.7 | [−15] | <2.0 | 5586 | <2.0 | 8041 | <0.02 | 83.7 | 18.4 | 7970 | 64.4 | 4.07 | $Na–SO_4–Cl$ | 38.88 |
| 38 | Lake Utinoe | D3 | 4 | – | 1 | 9.36 | 20.1 | 14.2 | [+80–90] | 1.33 | 1682 | <0.05 | 4042 | 0.34 | 240 | 43.6 | 2790 | 37.7 | 3.02 | $Na–SO_4–Cl$ | 6.53 |
| 41 | Lake Chernoe | C1+Q | 4 | – | 1 | 9.13 | 18.1 | 11.2 | [+150] | 1.68 | 617 | <0.05 | 530 | 1.45 | 30.1 | 33.3 | 797 | 4.98 | 0.52 | $Na–Cl–HCO_3–SO_4$ | 6.74 |
| 47 | Lake Solenoe | D3+C1 | 4 | – | 1 | 9.01 | 14.1 | 14.3 | [+80] | 3.21 | 1183 | <0.8 | 8607 | 0.38 | 306 | 112 | 4130 | 15.4 | 4.79 | $Na–SO_4$ | 2.56 |
| 48 | Lake Bulankul | K–O | 4 | – | 0 | 8.37 | 17.0 | 3.8 | [+120–130] | 1.51 | 5.58 | <0.05 | 0.91 | 0.40 | 23.0 | 26.7 | 14.7 | 4.53 | 0.031 | $Mg–Ca–HCO_3$ | 2.85 |
| 57 | Lake Ulugkol | C1 | 4 | – | 2 | 9.84 | 16.5 | 97.7 | [+50] | <2.0 | 7645 | <2.0 | 11052 | 0.05 | 178 | 4.21 | 11700 | 59.4 | 3.47 | $Na–SO_4–Cl$ | 465.25 |
| 58 | Lake Uskol | C1 | 4 | – | 1 | 9.93 | 15.8 | 80.1 | [0–+50] | 18.70 | 3471 | <2.0 | 10765 | 0.58 | 15.7 | 4.48 | 7560 | 20.2 | 4.49 | $Na–SO_4–Cl–HCO_3$ | 358.13 |
| 67 | Lake Vlasyevo | V–K/D1 | 4 | – | 0 | 9.24 | 18.0 | 20.3 | [+50] | 1.09 | 387 | 0.29 | 1333 | <0.02 | 309 | 21.9 | 626 | 31.8 | 0.47 | $Na–Mg–SO_4–HCO_3$ | 18.58 |
| 68 | Lake Shira (kurort) | D3 | 4 | – | 0 | 9.09 | 17.8 | 16.7 | [+65] | <2.0 | 2096 | 0.16 | 9765 | 0.74 | 1110 | 52.4 | 3320 | 37.3 | 2.12 | $Na–Mg–SO_4–Cl$ | 6.39 |
| 95 | Lake Shira 0.05 m | D3 | 4 | 0.05 | 0 | 8.86 | 17.8 | 18.3 | – | <2.0 | 2000 | <0.05 | 9625 | 0.76 | 1270 | 50.2 | 3701 | 39.3 | 2.25 | $Na–Mg–SO_4–Cl$ | 7.30 |
| 96 | Lake Shira 3 m | D3 | 4 | 3 | 0 | 8.90 | 17.3 | 17.7 | – | <2.0 | 2047 | <0.05 | 9862 | 0.77 | 1280 | 50.5 | 3707 | 39.3 | 2.27 | $Na–Mg–SO_4–Cl$ | 7.03 |

*(continued on next page)*

Table 1 (*continued*)

| No. | Location | Geology | Type | Depth (m) | $H_2S$ | pH | *T* (°C) | Alk (meq/L) | Eh (mV) | $F^-$ (mg/L) | $Cl^-$ (mg/L) | $NO_3^-$ (mg/L) | $SO_4^{2-}$ (mg/L) | Si (mg/L) | Mg (mg/L) | Ca (mg/L) | Na (mg/L) | K (mg/L) | B (mg/L) | Water type | Alk/Ca (meq/L) |
|---|---|---|---|---|---|---|---|---|---|---|---|---|---|---|---|---|---|---|---|---|---|
| 97 | Lake Shira 9 m | D3 | 4 | 9 | 0 | 8.92 | 7.9 | 19.9 | – | <2.0 | 2299 | <0.05 | 10627 | 1.67 | 1460 | 53.3 | 4190 | 44.1 | 2.54 | Na–Mg–$SO_4$–Cl | 7.49 |
| 98 | Lake Shira 13 m | D3 | 4 | 13 | 2 | 8.86 | 2.0 | 20.5 | – | <2.0 | 2331 | <0.05 | 10892 | 2.17 | 1470 | 54.0 | 4161 | 44.9 | 2.59 | Na–Mg–$SO_4$–Cl | 7.62 |
| 99 | LakeShira 18.4 m | D3 | 4 | 18.4 | 2 | 8.76 | 1.6 | 21.3 | – | <2.0 | 2401 | <0.05 | 10895 | 3.34 | 1410 | 53.3 | 4214 | 43.3 | 2.53 | Na–Mg–$SO_4$–Cl | 8.00 |

Geology: R, Riphean; K, Cambrian; O, Ordovician; K–O, Cambro–Ordovician granitoids; LPS, Precambrian or Lower Palaeozoic metasedimentary rocks; LPV, Precambrian or Lower Palaeozoic volcanics; D, Devonian; C, Carboniferous; Q, Quaternary; 1,2,3, lower, middle or upper, respectively.

Type: 1 = pumped borehole, 2 = artesian borehole, 3 = spring, 4 = lake, 5 = dug well, 7 = river/stream. Depth: Depth of well or borehole or depth of sampling in lake. $H_2S$ = hydrogen sulphide smell, 0 = absent, 1 = present, 2 = strong.

Brackets indicate determinations of dubious accuracy.

or artesian boreholes) or from regularly used pumped wells and boreholes, to ensure that samples were as representative as possible of in situ conditions. Pumped wells and boreholes were typically sampled from the tap nearest to the well-head, although in some cases water had passed through a water tower or header tank prior to the sample point. Information was seldom systematically available concerning groundwater levels or well construction.

Lake and river waters (with the exception of Xa95–99) were sampled by wading into the water body to a maximum depth of ca. 70 cm and by submerging sample bottles to a depth of some 20–30 cm and electrodes to a depth of some 5 cm below the water surface. For alkalinity titration, a clean bucket was filled with water and titrations performed on the shore. The samples from Lake Shira (Xa95–99) were collected from a boat in the centre of the Lake, using a remotely operated depth sampler, as described by Banks et al. (2001).

At each site, alkalinity was measured in the field (typically as an average of 3 determinations) using a portable acid titration test kit, using phenolphthalein or mixed/bromophenol blue indicators for p-alkalinity and t-alkalinity, respectively. Also, field determinations of pH, temperature and Eh (where turbulence and exposure to air were low enough to permit a meaningful reading) were made using relevant electrodes/thermistors and meters. Regular pH calibration was carried out using solutions of nominal pH 4, 7 and 10.

For chemical analysis, 100 ml polyethene flasks were rinsed with filtered water from the source to be sampled, and then filled with water filtered at 0.45 μm using a Millipore filter capsule mounted on a polypropene syringe. No field acidification/preservation was carried out. Sample flasks were transported by air to the laboratory of the Geological Survey of Norway in Trondheim, where they were stored in a cool room at 4 °C. The samples were treated and analysed as follows:

(i) The first sample quantum was analysed directly by ion chromatography (Dionex 120 DX) for inorganic anions ($SO_4^{2-}$, $NO_3^-$, $Cl^-$, $F^-$, $Br^-$, $PO_4^{3-}$).

(ii) The second sample quantum was acidified in the original flask using 0.5% concentrated Ultrapur $HNO_3$ to re-dissolve and hinder sorption or precipitation of poorly soluble elements. This acidified quantum was analysed for a wide range of elements by
- inductively coupled plasma atomic emission spectrometry (ICP-AES) on a Thermo Jarrell Ash ICP 61 (including Na, Mg, Ca, K, Si)
- and inductively coupled plasma mass spectrometry (ICP-MS) on a Finnegan Mat instrument with Meinhart Nebulizer CD-1.

(iii) In two cases (Xa57 and 58), field alkalinity proved too high for the field kits, and additional sample

flasks were returned to Norway for laboratory titration of alkalinity.

For all samples from the 1999 sampling, ion balance errors (IBE) were <10%, and almost all were <5%. For the 2000 sampling round, IBEs were less satisfactory (excess cations), especially for groundwater samples. There is some suspicion that field alkalinity determinations may have been underestimated, although by the time IBE was available, reanalysis of field alkalinity was impossible. Original determinations are thus presented in Table 1 and quality control data for results are presented by Banks et al. (2001).

Samples of evaporite crusts from lake shores and spring areas were taken in geochemical-grade paper sampling bags and analysed at the Norwegian University of Science and Technology (NTNU) by XRD on a Philips PW1710 diffractometer. In most cases, the evaporite crust was so thin that small quantities of soils and detrital materials could not be excluded from the sample.

## 5. Presentation and treatment of results

Analytical results are documented in full by Banks et al. (2001) and the most important parameters for analyses of water are summarised in Table 1. Modelling of speciation and saturation indices has been carried out by the codes MINTEQA2 (USEPA, 1991) for most of the waters and by PHRQPITZ v 1.11 (Plummer et al., 1988) for the most saline groundwaters and lake waters (Xa34, 38, 47, 57, 58, 59, 67, 68, 95–99). Results are presented graphically in two formats:

- as boxplots, showing the variation in statistical range of a parameter within a given subgroup (Fig. 5).

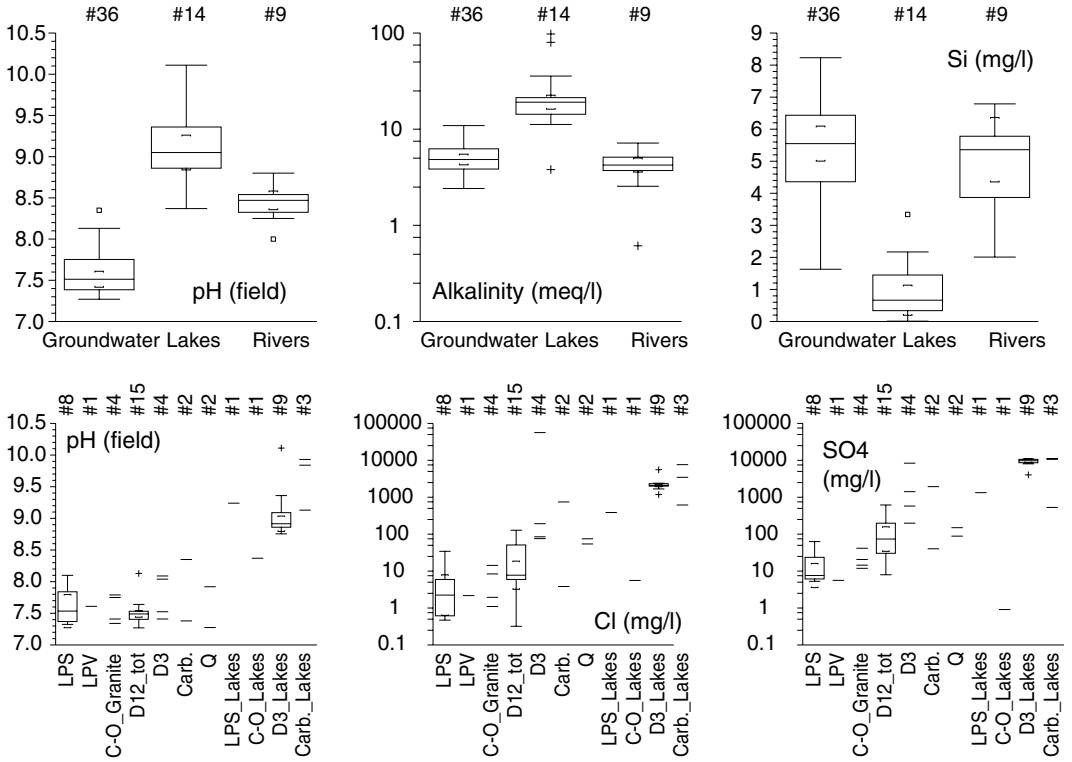


Fig. 5. Boxplots showing the range of variation of several hydrochemical parameters, sorted according to subset. The top 3 diagrams show distributions of pH, alkalinity and Si amongst subsets of groundwaters, river/stream waters and lake waters. The lower 3 diagrams show the distribution of pH, $Cl^-$ and $SO_4^{2-}$ amongst lithological classes (Groundwaters: LPS, Precambrian and Lower Palaeozoic metasedimentary rocks; LPV, Precambrian and Lower Palaeozoic volcanic rocks; C–O Granite, Cambro–Ordovician granitoids; D12_tot, Lower and Middle Devonian strata; D3, Upper Devonian strata; Carb., Carboniferous strata; Q, superficial Quaternary sediments. Lakes: same scheme applies, with suffix_Lakes). For each boxplot, # = number of samples; the box shows the inter-quartile range, with a horizontal line at the median value. "Whiskers" show the extra-quartile data, excluding near and far outliers, shown as squares and crosses, respectively. Horizontal "brackets" show 95% confidence interval around the median value. Results below detection limit are set to a value of half the detection limit for the purpose of statistical presentation.

- as *x*–*y* diagrams (Fig. 6). In most cases, species concentrations or saturation indices are plotted against $Cl^-$. Chloride, once dissolved, is assumed to act conservatively and to indicate the degree of up-concentration of solutes in the waters, either due to evaporite dissolution or to evapotranspiration.

Results of qualitative XRD analysis of neo-evaporite crusts or summarised in Table 2.

## 6. Water characterisation

This section of the paper describes and characterises the hydrogeochemistry of (a) groundwaters, (b) river waters and (c) lake waters in the study area. Note that, in this paper, the term "*evapoconcentration*" is used to describe the increase in concentration of soluble salts due to (a) direct evapotranspiration of recharge water from the soil/vegetation zone, (b) direct evapotranspiration of water from open water, spring areas or the root zone where the water table is shallow, and (c) the re-dissolution of neo-evaporite salts from the soil zone in recharging precipitation or in run-off to watercourses. The effects of these 3 processes cannot be distinguished in the current data set, but all lead to parallel, progressive concentration of salts until a mineral saturation ceiling is reached.

### 6.1. Groundwaters

The sampled groundwaters from this study exhibit broadly similar features to those sampled in the Shira area in the previous (1996) study and described by Parnachev et al. (1999b). They will thus not be described or considered in exhaustive detail, but the following features may be observed:

(i) The less saline samples tend to be dominated by Ca–(Mg)–$HCO_3$, the more saline ones by Na–$SO_4$–Cl (Table 1). There is, however, a significant

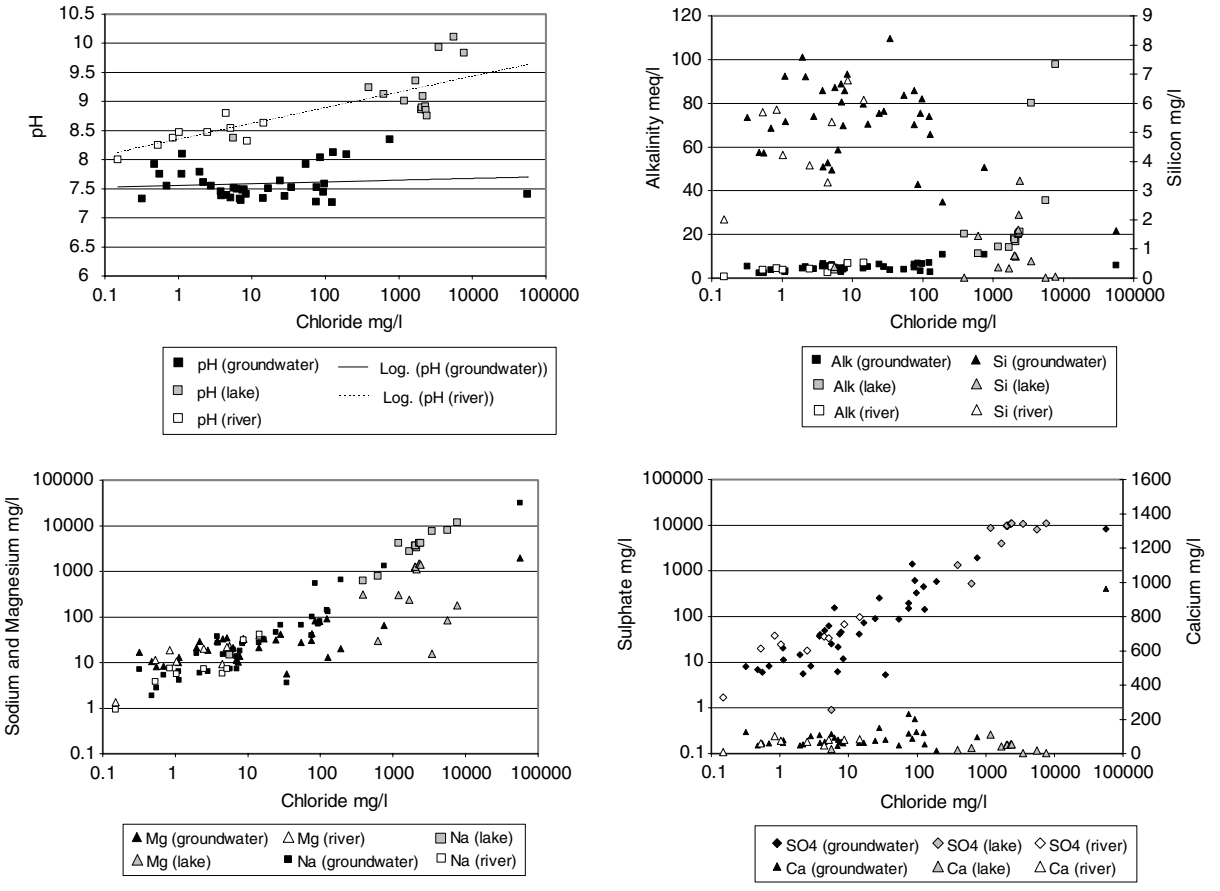


Fig. 6. (a) Concentrations of pH, alkalinity, Na, Mg, $SO_4$, Ca and (b) calculated saturation indices for the minerals calcite, gypsum, dolomite, chalcedony, halite, mirabilite, nesquehonite and sepiolite, plotted against Cl for sampled waters. In general, black symbols represent groundwaters, open symbols river waters and grey symbols lake waters. Saturation indices are calculated using MINTEQA2 for the majority of samples and PHRQPITZ for saline samples.

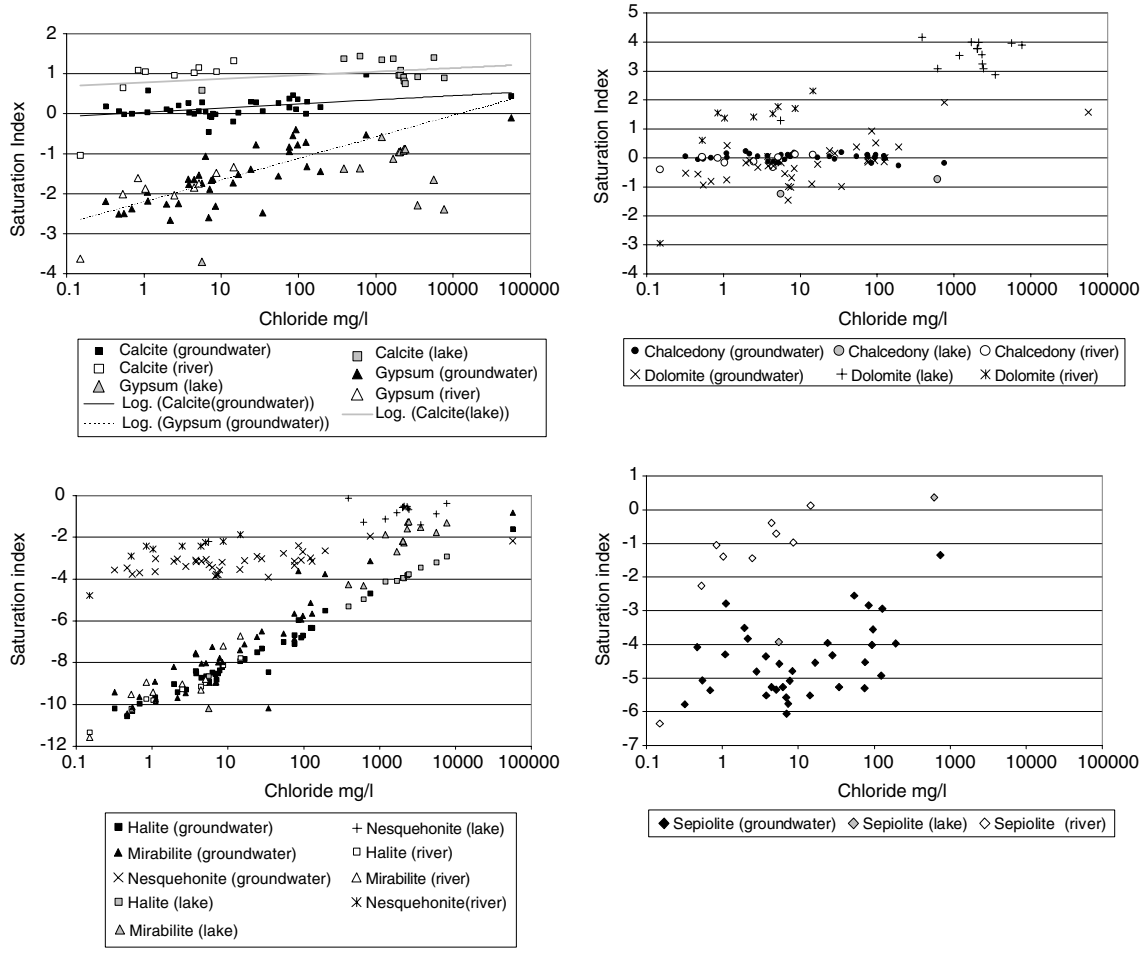


Fig. 6 (*continued*)

Table 2
Evaporite minerals identified by XRD in evaporite crusts at a groundwater seep in Devonian strata (Xa45), on the shores of saline lakes (Xa38, 41, 47, 57, 58) and in a dry saline lake bed near the Abakanskii salt well (Xa59)

| Sample No. | Xa45 | Xa38 | Xa41 | Xa47 | Xa57 | Xa58 | Xa59 |
|---|---|---|---|---|---|---|---|
| Locality | Spring area | Lake Utinoe | Lake Chërnoe | Lake Solenoe | Lake Ulugkol' | Lake Uskol' | Lake bed by salt well |
| Thenardite | √ | √ | √ | √ | √ | √ | √ |
| Mirabilite | 0 | √ | 0 | 0 | 0 | 0 | 0 |
| Calcite | √ | √ | √ | √ | √ | √ | √ |
| Dolomite | √ | 0 | 0 | √ | 0 | 0 | 0 |
| Gypsum | 0 | 0 | 0 | 0 | 0 | 0 | √ |
| Halite | 0 | 0 | 0 | √ | √ | √ | 0 |
| Rozenite (?) | 0 | 0 | 0 | 0 | 0 | √ | 0 |
| Ettringite (?) | √ | 0 | √ | 0 | √ | √ | 0 |

Thenardite, $Na_2SO_4$; mirabilite, $Na_2SO_4 \cdot 10H_2O$; rozenite, $FeSO_4 \cdot 4H_2O$; ettringite, $Ca_6Al_2(SO_4)_3(OH)_{12} \cdot 26H_2O$. √ = detected, 0 = not detected, ? = tentative mineral identification.

variation in water type, as will be noted from Table 1.

(ii) Sodium, $Cl^-$ and $SO_4^{2-}$ all increase approximately proportionately in groundwaters, suggesting that they are relatively conservative species and good indicators of solute accumulation by palaeo-evaporite (gypsum/halite) dissolution and, possibly, by "evapoconcentration" of recharge water and shallow groundwater (see above and Fig. 6).

(iii) pH values are all in the range 7.2–8.4 and show little significant trend with rock type (Fig. 5) or salinity (Fig. 6).

(iv) Alkalinity, Na, $Cl^-$ and $SO_4^{2-}$ all exhibit higher concentrations in the Devonian and Carboniferous rocks than in the Lower Palaeozoic rocks (Fig. 5). This is likely to be related to (a) the presence of evaporites in the Upper Palaeozoic sequence, (b) the greater degree of evapoconcentration of solutes in the lowland areas occupied by the Upper Palaeozoic, and (c) the greater degree of microbial productivity in lowland soils (leading to higher alkalinities). Topography is generally lower in the lowland Devonian and Carboniferous areas, resulting in slower groundwater flow and more hydrogeochemically "mature" groundwaters.

(v) Groundwaters are approximately saturated or slightly supersaturated with respect to calcite (Fig. 6). There is only a slight tendency to increasing calcite saturation index (SI) with $Cl^-$ salinity. Calcium and alkalinity concentrations do not vary greatly with salinity in groundwaters, suggesting that calcite saturation and precipitation is limiting Ca and $HCO_3^-$ accumulation in the waters.

(vi) Groundwaters are generally undersaturated with respect to gypsum (Fig. 6). Only two samples approach gypsum saturation, with SI$>-0.5$ (Xa88, Xa59). Gypsum SI increases in proportion to $Cl^-$ salinity, due to parallel accumulation of $SO_4^{2-}$ in the water.

(vii) Groundwaters are approximately saturated with respect to chalcedony (Fig. 6). Silicon concentrations are also relatively constant in groundwaters of low-moderate salinity, suggesting that silica saturation and precipitation acts as a control on Si accumulation in the waters. At high salinities, Si concentrations are lower in groundwaters, a feature that may conceivably be related to colloid formation and flocculation.

(viii) Groundwaters are typically undersaturated with respect to dolomite at very low $Cl^-$ salinity. However, as $Cl^-$ concentrations exceed 10 mg/L, approximate saturation is achieved, rising into supersaturation in more saline waters of $Cl^-$ $>100$ mg/L (Fig. 6). This supersaturation suggests that kinetic constraints on dolomite precipitation do not provide a rigid "dolomite saturation ceiling" to Mg concentrations. Magnesium exhibits increasing concentrations with increasing salinity, but not at the same rate as, say, Na.

(ix) Halite and mirabilite are undersaturated in all groundwaters (Fig. 6), although degree of saturation increases in proportion to $Cl^-$ salinity. The mirabilite SI is typically slightly higher than that for halite.

Especially in lowland areas, where the water table is close to the surface, such as spring areas, neo-evaporite (as opposed to Devonian and Carboniferous palaeo-evaporites) crusts and efflorescences may develop. XRD analysis of a sample of neo-evaporite crust from a seepage area near Moskovskii Sovkhoz (near sample Xa45) permitted the positive identification of thenardite, calcite, dolomite and, tentatively, the Ca–Al-hydroxy-sulphate ettringite.

The observations made above are entirely consistent with the evolutionary model outlined by Parnachev et al. (1999b) for the Shira region. In highland areas of Precambrian and Lower Palaeozoic rocks, standard groundwater evolutionary processes (carbonate and silicate weathering) prevail, yielding groundwaters of low salinity and Ca–$HCO_3$ composition. In lower areas, lower rainfall and higher evapoconcentration, coupled with dissolution of palaeo-evaporite minerals (gypsum, halite) from Upper Palaeozoic deposits of the Minusinsk trough, result in progressive accumulation of $Cl^-$, $SO_4^{2-}$ and Na in the groundwater. Calcite saturation in the presence of significant alkalinity prevents accumulation of Ca in the waters and thus also prevents gypsum saturation from being achieved, allowing $SO_4^{2-}$ to accumulate in the water. Calcite precipitation also buffers pH and maintains it in a slightly alkaline condition. Supersaturation with respect to dolomite suggests kinetic constraints on dolomite precipitation. Nevertheless, Mg does not increase with salinity as fast as, for example, Na, suggesting some sink for Mg within the groundwater system. Sepiolite is generally undersaturated in groundwater samples, although chalcedony is typically saturated, suggesting that silica is the major controlling phase for Si in groundwaters (Fig. 6).

### 6.2. River waters

The stream and river waters sampled are generally of low to moderate $Cl^-$ content, ranging from 0.15 mg/L $Cl^-$ in the River Bolshoi On (Xa74; in the mountains, comprised of pre-Minusinsk basement, along the border with Tuvan Republic) to 14.5 mg/L in the River Son near Lake Shira. The extremely low $Cl^-$ concentrations in the upper reaches of streams reflect the distance from the sea and consequent lack of marine aerosols in precipitation. Concentrations of both Na and $SO_4^{2-}$ generally exceed $Cl^-$ in stream waters, probably reflecting the

redistribution of $Na_2SO_4$ in soils and lakeside evaporites both by atmospheric transport of dust and direct leaching from soils and neo-evaporite crusts at groundwater discharge areas. In this context, the ubiquitous presence of the $Na_2SO_4$, thenardite, in the sampled neo-evaporite crusts, compared with the sporadic presence of halite, should be noted (Table 2). River and stream waters are, however, generally dominated in their ionic composition, by Ca and $HCO_3^-$ (Table 1).

In most of the plots of salinity-related trends (Fig. 6), river and stream waters generally coincide with the groundwater "envelope", with the following exceptions:

(i) Despite having similar Ca and alkalinity concentrations, river and stream waters generally exhibit higher pH values (typical range 8–9) than groundwaters (Table 1, and Figs. 5 and 6).
(ii) Saturation indices for mirabilite, halite, chalcedony and gypsum are generally similar to those for groundwaters of similar salinity (Fig. 6). Saturation indices for calcite and dolomite are generally significantly higher, often displaying considerable supersaturation. These elevated saturation indices are related to the elevated pH values of the streams (Ca, alkalinity and Mg concentrations being broadly similar to the groundwaters).
(iii) The degree of supersaturation achieved by calcite and dolomite suggests non-equilibrium conditions. In other words, pH rises are achieved more rapidly (by equilibration with the atmosphere, and by evaporative concentration) in these relatively fast-flowing surface water systems than the supersaturated minerals can precipitate.
(iv) Sepiolite approaches saturation (Fig. 6), especially in some of the more saline surface waters, suggesting that it may be a plausible controlling phase for Si concentrations in solution.

In temperate climates, it is common to expect groundwater pH values to be higher than those in surface waters, as the latter often contain a high proportion of surface run-off and interflow, with a low degree of pH-buffering by water–rock interaction. In semi-arid Khakassia, the opposite appears to be true: streams are largely fed by groundwater baseflow for much of the year and exhibit higher pH values.

To assist in the understanding of the processes taking place in Khakassian streams, the River Son has been sampled at 4 localities along its length. Lake Shira (into which it discharges) has also been sampled. Fig. 7 shows how concentrations of solutes change along the length of the Son. The following points may be noted:

(i) pH is already relatively high (8.25) at the upstream sampling point. There is a tendency to a gradual increase downstream to a pH of around 8.8 in Lake Shira.
(ii) Chloride shows a systematic increase downstream, most likely indicative of evaporative concentration. Estimates suggest that evaporation from the River Son channel alone (neglecting tributaries and spring areas) could reach 5–10 L/s in summer: a potentially significant figure in such a relatively minor river, whose channel is only some 2 m wide for much of its length.
(iii) Between Sonskii and Katjushkino, both $NO_3^-$ and $Cl^-$ exhibit a significant rise, possibly suggestive of an influx of waste effluent (at Sonskii town?). Downstream of Katjushkino, $NO_3^-$ concentrations decline, indicating either dilution by uncontaminated water or denitrification.
(iv) From the upper part of Fig. 7, where concentrations are normalised to unity at the upstream sampling point, Na also shows progressive accumulation (presumed to be via evapoconcentration) downstream, followed by $SO_4^{2-}$, Mg and Sr (in that order).
(v) Alkalinity shows a lower, but recoganisable, progressive increase downstream.
(vi) Calcium shows a low degree of concentration downstream, suggestive of some precipitation of $CaCO_3$ limiting Ca accumulation in solution. Calcium concentrations actually decrease in Lake Shira.
(vii) There is little increase in Si concentrations in the River Son, and a substantial decrease in Lake Shira. This is likely due to the precipitation of silica (e.g., chalcedony) or a silicate (e.g., sepiolite) phase, or to the biotic removal of silica (for example, in diatoms).

### 6.3. Lake waters

Many of the lakes in Khakassia have a stratified composition, with a thermocline and an oxycline. An example of this is Lake Shira (Fig. 8). With the exception of the samples from Lake Shira (Xa95–99), the lake waters sampled during this study are of summer surficial waters, typically near the lake shore. As such, they are unlikely to be wholly representative of the lake composition. Indeed, at most of the lowland lakes, the bottom sediments are highly reducing, with measured Eh values in the immediate subsurface of the substrate typically between −400 and −200 mV. $H_2S$ odours were detected at Lakes Kurinka, Utinoe, Chërnoe, Solenoe, Ulugkol', Uskol' and in deeper samples from Lake Shira, confirming the presence of $SO_4^{2-}$ reduction processes in the lakes.

However, if discussion is restricted to the sampled portions of the lakes, a considerable variation in composition is observed. The least saline lake sampled (5.58 mg/L $Cl^-$) was Lake Bulankul' (Xa48), at elevated altitude and located on pre-Devonian basement. Bulankul' also has a lower pH than the other lakes (8.37), a relatively low alkalinity (3.8 meq/L) and one of the higher

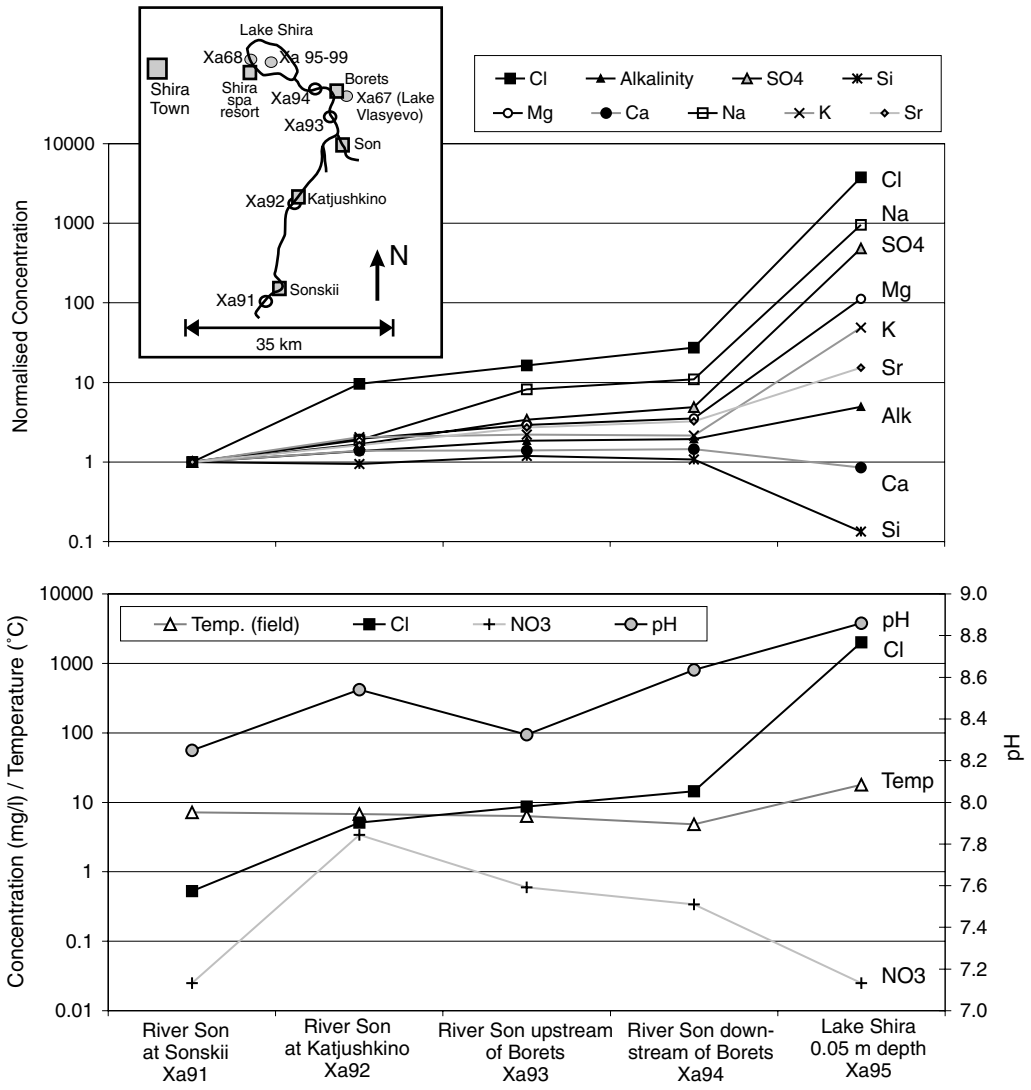


Fig. 7. Diagrams showing variations in major ion chemistry along the length of the River Son (samples Xa91 to 94, from the left) to Lake Shira (sample Xa95). (a) sketch map of sampling locations (circles) and towns (squares), (b) concentrations normalised to the initial upstream sampling point (Xa91), (c) shows absolute concentrations of $Cl^-$ and $NO_3^-$, together with temperature and pH.

Eh values (around +125 mV). The water type is Mg–Ca–$HCO_3$.

The other sampled lakes are located on Devonian or Carboniferous strata and are generally topographically lower. They have pH values in excess of 9.0, generally low Eh values (range −15 to +150 mV), high alkalinities (>10 meq/L) and moderate to high $Cl^-$ and $SO_4^{2-}$ salinity (ranging from 387 mg/L Cl in Lake Vlasyevo to 7645 mg/L in Lake Ulugkol', and from 530 mg/L $SO_4$ in Lake Chërnoe to 11,050 mg/L in Lake Ulugkol'). The waters of these lakes tend to be dominated by Na and Mg as cations, and $Cl^-$ and $SO_4^{2-}$ as anions. The two lakes of rather modest salinity (Chërnoe and Vlasyevo) also exhibit a significant $HCO_3^-$ component.

The lowland lake waters are generally more saline than the river waters due to significant evapoconcentration (note the large difference in solute concentrations between the River Son and Lake Shira in Fig. 7), and also than most of the groundwaters (and the most saline groundwater, Xa59, comes from a salt well in an old lake bed). Magnesium, Na, K and $SO_4^{2-}$ concentrations in lake waters lie broadly on the same trend lines as ground- and river water samples (Fig. 6). Like the river waters, the lake waters exhibit substantially higher pH values and pH-related saturation indices (calcite, nesquehonite, dolomite) than groundwaters. Lake water pH values appear to plot on the same trend line as river waters (one tending towards a gradual increase in pH with salinity).

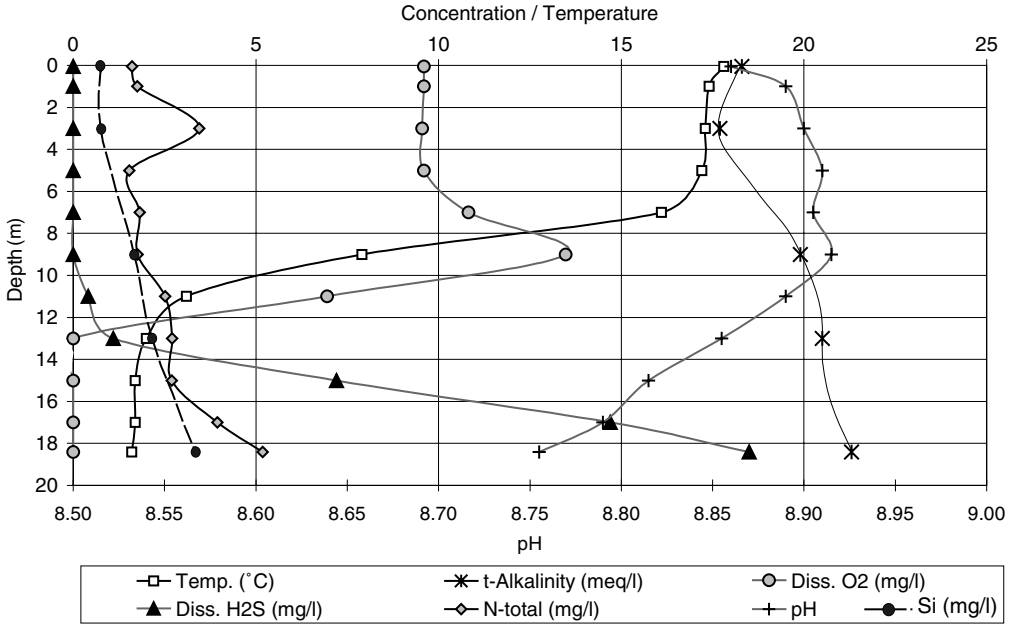


Fig. 8. Hydrochemical depth profiles near the centre of Lake Shira, showing concentrations of alkalinity, $H_2S$, dissolved $O_2$, total N (which is essentially equivalent to ammoniacal N), temperature, Si and pH, plotted against depth (m). Data are derived from Banks et al. (2001).

Compared with both river waters and groundwaters, lake waters are relatively depleted in Ca and Si (see alkalinity/Ca ratios in Table 1). It appears that elevated alkalinities and pH result in Ca removal via calcite precipitation (see Fig. 7). Removal of Ca in turn depresses the gypsum saturation index relative to its groundwater trend. The low Si lake water concentrations (especially in the upper part of the lakes, Fig. 8) are likely to be due to the biotic precipitation of silica (e.g., in diatom tests) or precipitation of a silicate (e.g., sepiolite) phase that becomes saturated in the most saline waters.

Often, thin evaporite crusts are found around the lake shores. These may be formed by evaporation of lake water spray, or be efflorescences formed by evaporative wicking of saline waters in the immediate subsurface. Sampling (Table 2) confirms that thenardite and calcite are ubiquitous in these crusts, with halite only being present in some samples.

## 7. Modelling evolution of surface waters from groundwater

Fig. 6 suggests that systematic trends can be identified in the rather sparse and variable Khakassian data set that seem to point towards real evolutionary mechanisms. As a working hypothesis, it is proposed that:

(i) Immature highland groundwaters are dominated by Ca, Mg and $HCO_3^-$ ions resulting from carbonate and silicate weathering reactions. In lowland areas, evapoconcentration in the soil zone and dissolution of palaeo-evaporites (e.g., halite, gypsum) progressively increases salinity, eventually leading to precipitation of calcite and a Na–$SO_4$–Cl groundwater chemistry.

(ii) River and lake waters evolve from groundwater baseflow largely by means of evapoconcentrative processes (direct evapo(transpir)ation and dissolution of neo-evaporites), coupled with progressive removal of mineral phases as saturation ceilings are reached.

Parnachev et al. (1999b) have demonstrated the plausibility of (i), the groundwater evolution pathway. This section employs hydrochemical modelling to demonstrate the plausibility of (ii), the mechanism for evolution of river and lake waters from groundwater baseflow. Any plausible model must be able to simulate the following features:

- the progressive dominance of Na, $SO_4$ and $Cl^-$, over Ca and $HCO_3^-$,
- the elevated pH of surface waters,
- the stable Si concentrations at low-moderate salinity, and their decrease at elevated salinity.

As starting points, for the hydrochemical modelling, two groundwater samples have been selected that could

potentially be representative of baseflow feeding surface water systems:

(i) Sample Xa45, from a spring area SW of Moskovskii Sovkhoz in Lower Carboniferous strata. The area is characterised by saline efflorescences in the soil and black, reducing channel bed sediments.
(ii) Sample Xa66, from a borehole in Lower Devonian basalts and sandstone at Polindeika.

Both groundwaters have good ion balances (errors <5%), slightly alkaline pH values (8.35 and 8.13) and are moderately saline (747 and 128 mg/L $Cl^-$, respectively). Taking the major ion ($Na^+$, $Ca^{++}$, $K^+$, $Mg^{++}$, alkalinity, $SO_4^{2-}$, $Cl^-$ and Si) composition of these waters as a starting point, PHREEQC Interactive version 2.5 (Parkhurst, 1995) was used to simulate the evaporative concentration of the 1 L of water by the removal of 52.73 moles (for Xa45) or 55.00 moles (for Xa66) of water in 40 steps (i.e., 95–99% of water removed). This concentration factor is regarded as plausible for relatively closed systems (such as some soil reservoirs or lakes), given that annual potential evapotranspiration exceeds rainfall over much of the lowland area of Khakassia. At each step, the solution was equilibrated with a partial $CO_2$ pressure of $10^{-3.5}$ atmospheres (i.e., approximately atmospheric). The following mineral phases were allowed to precipitate out when (and if) they became oversaturated: mirabilite, chalcedony, gypsum and halite. In different runs of the model, precipitation of sepiolite or calcite was either permitted or suppressed.

PHREEQCI purports to use activity algorithms that are valid up to ionic strengths approximately corresponding to those of sea water. Thus, the very last steps of the modelling runs (which reach $Cl^-$ concentrations of almost 15,000 mg/L) considered below are of dubious validity. Thus, the less flexible but, strictly speaking, more valid code PHRQPITZ v. 1.11 (Plummer et al., 1988) was used to check selected individual concentration steps by titrating Xa45 with negative amounts of pure water. No serious deviations from the trends indicated by PHREEQCI were identified (although minor deviations were unavoidable due not only to differing activity algorithms, but also to differing thermodynamic data in the databases and the limited number of mineral phases available to PHRQPITZ).

### 7.1. Modelling results

Selected modelling results are shown for both initial water compositions in Fig. 9. In both waters, there is an initial abrupt increase in pH during the first step of the model run, representing equilibration of the groundwater with the lower partial $pCO_2$ of the atmosphere by degassing of $CO_2$. This process affects pH but not alkalinity, as pointed out by Appelo and Postma (1996)

$$HCO_3^- = CO_2 + OH^-$$

Subsequently, in both models, pH shows a steady rise due to the common ion effect of $H^+$ and $OH^-$. As the solution is concentrated, concentrations of both ions would increase, exceeding the dissociation product of water. Thus, equal amounts of the two ions recombine to produce water molecules but, as there was initially an excess of $OH^-$ over $H^+$ (initially alkaline solution), the relative excess of $OH^-$ increases and pH rises. At the end of the run (corresponding to $Cl^-$ concentrations in the range 14,000–14,900 mg/L), pH values of 9.7–9.8 are achieved if calcite is not permitted to precipitate. Slightly lower final pH values are attained if precipitation of calcite is permitted, due to the buffering effect of this reaction

$$Ca^{++} + HCO_3^- = CaCO_3 + H^+$$

For sample Xa45, both initial $SO_4^{2-}$ and alkalinity concentrations greatly exceed initial Ca concentrations (as meq/L). In all modelling runs, Na, Mg and $SO_4^{2-}$ increase in proportion to $Cl^-$. If calcite precipitation is *not* permitted, Ca concentrations increase until gypsum saturation is achieved, at which point Ca concentrations stabilise. Sulphate is not significantly affected by gypsum precipitation due to its great excess over Ca. Alkalinity accumulates in solution until, at the end of the run, concentrations of 96 meq/L are achieved. If calcite precipitation is permitted, Ca is progressively removed from solution with increasing evaporation. Gypsum saturation is not attained. Alkalinity accumulates (but at a reduced rate), and reaches a concentration of 58 meq/L. The resultant water at step 40 is of Na–$SO_4$–Cl type.

For sample Xa66, initial $SO_4^{2-}$ and alkalinity are only slightly greater than Ca (as meq/L). When calcite precipitation is not permitted, alkalinity and Ca accumulate approximately in parallel with $Na^+$, $Mg^{++}$ and $Cl^-$, with alkalinity reaching a value in excess of 100 meq/L by the end of the run. Gypsum saturation is eventually reached around Step 38, reducing the rate of increase of both Ca and $SO_4^{2-}$ ions. The resultant water is of Na–Ca–Mg–Cl–$SO_4$–(H)$CO_3$ type. When calcite precipitation is permitted, the common ion effect results in Ca being removed from solution and alkalinity accumulating (albeit at a lower rate than $Cl^-$) to reach a value of around 10 meq/L by end of run. Gypsum saturation is not attained. The resultant water at the end of the run is of Na–Mg–Cl–$SO_4$ composition.

For both initial water compositions, if sepiolite precipitation is not permitted, the solution becomes saturated with respect to silica (chalcedony), which maintains dissolved Si concentrations at a relatively stable value. When sepiolite precipitation is permitted, however, it has little effect on Mg concentrations (as

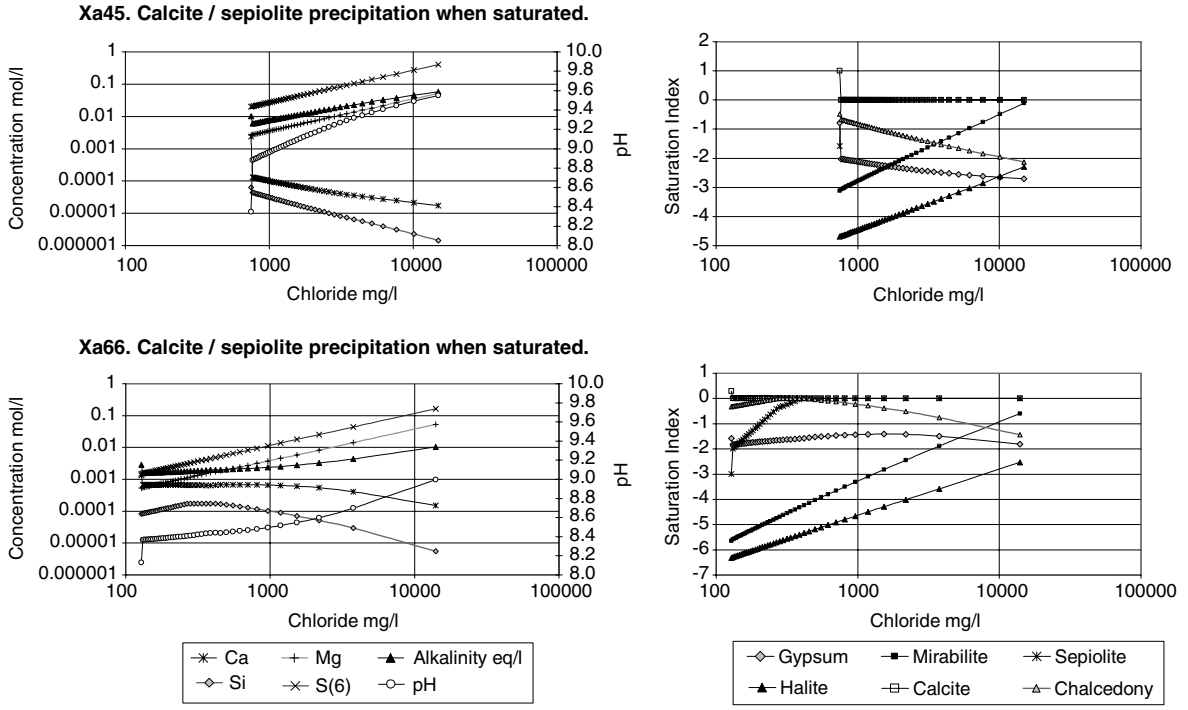


Fig. 9. Modelled evaporative concentration of groundwater samples Xa45 and Xa66, in equilibrium with a partial $CO_2$ pressure of $10^{-3.5}$ atm., using the code PHREEQC Interactive, in 40 steps. Diagram (a) excess calcite, sepiolite, chalcedony, halite, mirabilite and gypsum are allowed to precipitate when saturated; Diagram (b) precipitation of calcite and sepiolite are not permitted. The left hand diagrams show the evolution of modelled concentrations of solutes with increasing $Cl^-$. The right hand diagram shows the evolution of mineral saturation indices. Alkalinity is calculated as the milliequivalent sum of $HCO_3^-$, $CO_3^{2-}$ and $OH^-$.

these greatly exceed Si), but does result in decreasing Si concentrations in the more saline stages of evolution.

During all modelling runs, the solutions remain undersaturated with respect to both halite and mirabilite, although mirabilite saturation is almost attained on the final step of the model runs for Xa45.

## 8. Discussion

The hydrochemical modelling tools employed in this study are not complex: they simulate the evapoconcentration of initial groundwater compositions, and permit the precipitation of selected mineral phases. This section assesses whether such simplistic models adequately represent the processes seen to be occurring in the real data set.

Results indicate that, when calcite precipitation is allowed, the modelling does successfully simulate the salinization process, with Na, $SO_4^{2-}$ and $Cl^-$ accumulating in the water preferentially over alkalinity and (especially) Ca. Additionally, the calculated saturation indices evolve similarly in modelled and real data: halite remains undersaturated in all waters up to the salinities observed in the field; mirabilite reaches approximate saturation only in the most saline waters; and gypsum remains undersaturated at most salinities when calcite precipitation is allowed. Furthermore, the model yields pH values similar to those observed in the real Khakassian lake water data (pH 9–10). Modelling also simulates the relatively constant Si concentrations, with (when sepiolite precipitation is allowed) declining concentrations in the most saline water samples.

The modelling runs that permit calcite precipitation demonstrate the Hardie and Eugster (1970) concept of saline surface water evolution that invokes the common ion effect to explain how initial water compositions "roll off" hydrochemical "watersheds" during evapoconcentration, eventually gravitating towards a limited number of final compositions. Hardie and Eugster's (1970) first hydrological "watershed" is represented by calcite saturation and precipitation. If Ca exceeds alkalinity (as meq/L) in the initial solution, alkalinity will decrease in solution and Ca accumulate. If alkalinity exceeds Ca (as in the modelled waters, here), Ca is removed and alkalinity accumulates. In Xa66, the initial solution is more dilute and the concentrations of Ca and alkalinity more

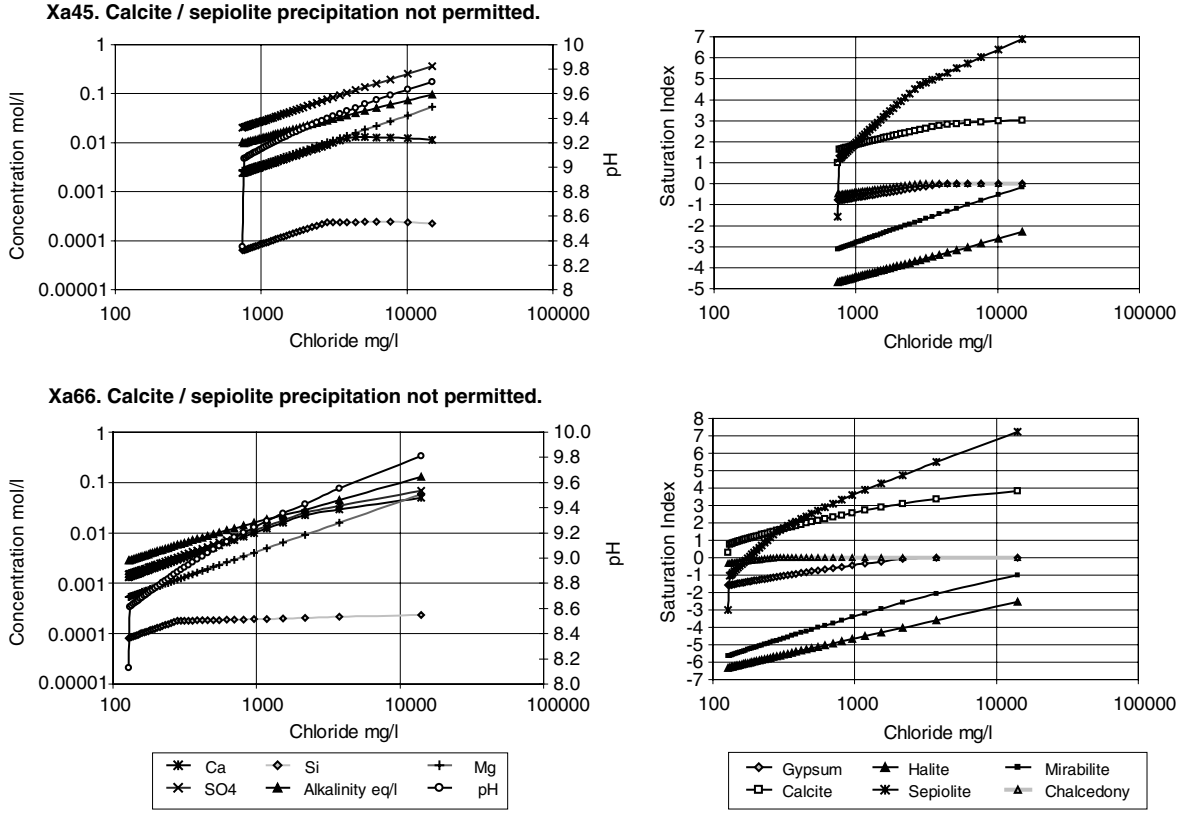


Fig. 9 (*continued*)

nearly equal than in Xa45. Thus, during evapoconcentration, Xa66 takes longer to roll "off" the calcite "watershed".

Table 3 demonstrates that modelling not only reproduces the trends seen in real hydrochemical data, but also yields final concentrations of major ions that are consistent with those observed in the sampled saline lakes. Only minor discrepancies are noted in Table 3. For example, maximum alkalinities, and Ca concentrations are slightly higher than those predicted by the models that incorporate calcite precipitation. This observation simply reflects the rigid saturation limit ($SI = 0$) used in the model to control calcite precipitation, as opposed to the observed fact that real calcite SIs exceed zero, presumably due to kinetic factors.

The one aspect of the real data sets that modelling fails to adequately simulate is the evolution of Mg concentrations. In the modelled results (Fig. 9), Mg

Table 3
Results (at Step 40) of PHREEQCI modelling of evaporative concentration of initial groundwater compositions from sample points Xa45 and Xa66, with calcite and sepiolite precipitation allowed, compared with the range of real lowland lake water concentrations observed in the field

| | Modelled Xa45 Step 40 | Modelled Xa66 Step 40 | Real lowland lake water data |
|---|---|---|---|
| Ca (mg/L) | 1 | 6 | 4–112 |
| Na (mg/L) | 26,300 | 14,500 | 630–11,700 |
| Mg (mg/L) | 1280 | 1290 | 16–1470 |
| Alkalinity (meq/L) | 58 | 10 | 11–98 |
| $SO_4^=$ (mg/L) | 38,700 | 15,600 | 530–11,100 |
| $Cl^-$ (mg/L) | 14,900 | 14,000 | 390–7600 |
| pH | 9.6 | 9.0 | 8.8–10.1 |
| Si (mg/L) | 0.04 | 0.16 | <0.02–3.3 |

accumulates in parallel to Na and Cl, whereas the real data (Fig. 6) suggest that Mg accumulates at a considerably reduced rate compared to, say, Na.

### 8.1. Evolution of Mg concentrations

The models described above have not considered dolomite precipitation, largely because significant dolomite supersaturation is observed in the real surface water analyses (SI = 1–4), suggesting that kinetic factors negate dolomite precipitation as a control on Mg concentrations.

A further possible explanation for the apparent suppressed rate of Mg accumulation in saline waters is sepiolite precipitation. Indeed, sepiolite precipitation would be the second "hydrochemical watershed" expected to be encountered by our waters according to Hardie and Eugster (1970) (discussed further by Appelo and Postma, 1996)

$$Mg^{2+} + 3SiO_2 + 2HCO_3^- = MgSi_3O_6(OH)_2 + 2CO_2$$

According to the Hardie and Eugster concept, if alkalinity (in meq) exceeds Mg (as it does in Xa45 and Xa66), Mg is removed from solution by the common ion effect and an alkaline Na–$HCO_3$–$SO_4$–Cl brine results. If Mg exceeds alkalinity, a Na–Mg–$SO_4$–Cl water results. It should be noted that, in neither the modelling run for Xa45 nor that for Xa66, does sepiolite saturation represent the hydrogeochemical watershed that the Hardie and Eugster concept predicts. In fact, both Mg and alkalinity continue to accumulate in solution. The reason for this appears to be that dissolved Si concentrations (ultimately controlled by silica saturation) appear to limit the amount of sepiolite that can be precipitated. As the initial Si concentrations are very much less than those of Mg and alkalinity, sepiolite precipitation has little effect on these components and merely serves to remove Si from solution. Field data appear to support this interpretation, as both Mg and alkalinity appear to accumulate in surface waters with increasing salinity (Fig. 7(a)), with depleted Si in the most saline waters. It is thus concluded that sepiolite precipitation alone does not provide an adequate explanation for the suppressed rate of Mg-accumulation in saline solutions.

A final explanation is that Mg is co-precipitated with Ca in high-Mg calcite, rather than pure calcite. In the modelling runs without calcite precipitation, Ca accumulates to between 500 and 2000 mg/L by Step 40 (end of run). When calcite precipitation is allowed, Ca concentrations reach as low as 1–6 mg/L. Models predict concentrations of Mg of 1300–1400 mg/L by Step 40 of the model run. Concentrations of this order of magnitude are seen in Lake Shira, but are more typically 100–300 mg/L in the saline lakes (Table 1). If it is assumed that the molar ratio of Mg/Ca in high-Mg calcite is 0.15, implying a mass ratio of around 0.1, precipitation of high-Mg calcite could only account for a suppression in accumulated Mg concentration of 50–200 mg/L. It is thus concluded that precipitation of high-Mg calcite alone is also insufficient to account for the suppressed rate of Mg accumulation in surface waters.

Further explanations could be proffered, such as progressive dolomitization of precipitated calcite, ion exchange, precipitation as, or sorption onto, silicate phases, but none of these are rigorously testable using the existing data set.

### 8.2. Biological processes

While the simple hydrochemical evapoconcentrative model described above appears remarkably powerful in explaining many features of the major ion hydrochemistry, it is recognised that less tractable biological processes may also be important in modifying water composition, especially in the lowland saline lakes. Eh measurements and the presence of $H_2S$ testify to the presence of bacterial $SO_4^-$ reduction processes in the waters and substrates of most of the lakes. Vertical profiling of Lake Shira indicates both the presence of a thermocline and a strong redox gradient. The upper portion of the lake is oxic and devoid of $H_2S$ (with a peak in dissolved $O_2$ marking the point of optimum microbiological photosynthetic activity), while the lower portion of the lake is characterised by dissolved sulphide and $NH_4^+$, and the absence of oxygen (Fig. 8). Biotic precipitation of silica by diatoms may also be a further mechanism for removal of Si from solution in the upper part of the lake.

## 9. Conclusions

Samples of ground-, river and lake water have been collected from the semi-arid, southern Siberian Republic of Khakassia. Despite the fact that the samples have not been collected from a single evolutionary flow path, or necessarily from a single hydrological unit, presentation of salinity-related trends in concentrations and saturation indices within the data set does allow meaningful conclusions to be drawn about the most important hydrochemical evolutionary processes occurring in the area.

As regards groundwater, the least saline samples are derived from "basement" areas of Lower Palaeozoic metasediments, metavolcanics and plutonic rocks. Not only will these silicate-dominated lithologies have slow water–rock interaction kinetics, they tend to form higher ground and be subject to higher precipitation rates. They thus occupy the initial portions of regional groundwater flow pathways and will have generally lower residence times. The more saline groundwater

samples are derived from Upper Palaeozoic volcano-sedimentary basin infill lithologies of the Minusinsk depression. These occupy generally lower-lying and more arid areas, and are characterised (especially in the Upper Devonian) by the presence of palaeoevaporite minerals such as gypsum and halite. While less saline groundwaters are dominated by Ca–$HCO_3^-$ hydrochemical type, saline groundwaters are characterised by Na–Cl–$SO_4$. The groundwater data from this study support the conclusions drawn by Parnachev et al. (1999b) from an earlier study of the Shira area, namely that groundwater salinity evolves by processes dominated by dissolution of minerals such as gypsum and halite in the presence of alkalinity (e.g., generated by silicate weathering). The presence of alkalinity serves to maintain calcite saturation, and suppress Ca accumulation in solution and hence prevent gypsum saturation. The relatively low (circum-neutral) pH of groundwaters and the lack of salinity-related pH trends, suggests that evolution of groundwater salinity occurs in the subsurface rather than during exposure of groundwaters to the atmosphere. The presence of evaporite efflorescences on soils in areas of high water table suggests that evaporative wicking may be a contributory mechanism to evolution of groundwater salinity in lowland areas.

In the lower-lying, semi-arid areas of Khakassia, groundwater baseflow is likely to provide the dominant contribution to surface watercourses throughout much of the year. The river and stream waters sampled (in dry summer months) do, in fact, display a major ion hydrochemistry that is broadly similar to groundwater, with the exception that pH is significantly higher in the surface water. Sampling along the length of the River Son indicates that river water is subject to progressive downstream evapoconcentration (a term taken to include both direct evaporation, and redissolution of neo-evaporite saline crusts and soil salts in run-off) and that pH increases gradually as salinity increases. Lowland saline lake waters essentially represent the terminal stages of hydrochemical evaporative evolution of surface waters and generally lie on hydrochemical trends extrapolated from river and stream waters. In the most saline lake waters, pH values of 9–10 and a Na–$SO_4$–Cl composition are reached, while Ca and Si concentrations are depleted.

Simple modelling has been carried out using PHREEQCI to simulate the evolution of groundwater baseflow towards lake water. It is demonstrated that most aspects of major ion chemistry can successfully be simulated by invoking only 5 main mechanisms:

(i) *Equilibration with atmospheric $CO_2$*, resulting in degassing of $CO_2$ from groundwater and a rise in pH (observable in river water when compared with groundwater).
(ii) *Evapoconcentration*, resulting in gradual, parallel accumulation of $Cl^-$, $SO_4^{2-}$ and Na in solution, and to a lesser extent alkalinity. The common ion effect of $H^+$ and $OH^-$ means that evapoconcentration of waters with an initial $OH^-$ excess will result in an increasing excess of $OH^-$ over $H^+$ and final pH values in the range 9–10.
(iii) *Precipitation of calcite* from waters where initial alkalinity exceeds Ca concentration, resulting in Ca being progressively removed from solution. Alkalinity accumulates, but at a reduced rate (see (ii) above). In the real surface waters, calcite is often supersaturated. Thus, although calcite precipitation constrains dissolved Ca concentrations, the precipitation process is too slow to keep pace fully with evaporative concentration.
(iv) *Chalcedony saturation and precipitation*, limiting concentrations of Si which can accumulate in groundwater and surface water.
(v) *Sepiolite saturation* and precipitation in the most saline lake waters, resulting in removal of Si from solution.

The one aspect of the real data that the model cannot simulate is the apparently reduced rate of Mg accumulation in saline waters (compared with, for example, Na). No single mechanism seems adequate to explain this phenomenon fully: sepiolite precipitation is limited by Si availability; dolomite precipitation appears to suffer from kinetic constraints, while precipitation of high-Mg calcite is quantitatively insufficient. It appears necessary to invoke more than one of these processes to explain the evolution of the observed Mg-trend, possibly coupled with others which are not readily simulated, such as ion exchange of Mg, or dolomitization of calcite precipitates.

Both modelling and empirical data suggest that saturation with respect to sodium sulphate (e.g., mirabilite) and gypsum are only approached in the ultimate phases of evaporative concentration in the Khakassian environment. Halite remains unsaturated. Thenardite, calcite and, occasionally, halite and ettringite are observed in thin evaporite crusts surrounding lake shores and probably produced either by evaporation of lake spray or evaporative wicking of shallow lakeside subsurface brines.

## Acknowledgements

The authors thank the British Council (Moscow) and the Norwegian University of Science and Technology (Trondheim) for funding international participation in the Russian fieldwork. The Geological Survey of Norway kindly provided water analyses. I.I. Vishnivyetskii (Chairman of the Committee for Environmental Pro-

tection of the Khakassian Republic, Abakan) is thanked for his fruitful co-operation and provision of transport. The authors also thank A.A. Bulatov (Committee for Natural Resources of the Khakassian Republic, Abakan), A.G. Degermendzhii and N.A. Gaevskii (Institute of Biophysics; Siberian Branch of the Russian Academy of Sciences, Krasnoyarsk), N.A. Makarenko and A.Y. Berezovskii (Tomsk State University), Y.M. Dutova and S.L. Shvartsev (Tomsk Polytechnic University), D.S. Pokrovskii (Tomsk State Architecture and Buildings University), Igor and Vera Seryodkin, Andrei Zverev, Natasha Zvereva, Valya Vilnina and many other friends and colleagues in Tomsk and Khakassia for their assistance and hospitality. Dr. Tim Atkinson and two anonymous referees are thanked for their reviews of the first version of this manuscript.

## References

Appelo, C.A.J., Postma, D., 1996. Geochemistry, groundwater and pollution (3rd corrected print). Balkema, Rotterdam/Brookfield.

Balakhchina, N.P., Orlova, L.P., Butanaev, V.Y., Kozodoev, M.S., Kustov, Y.I., Kizlasov, I.L., Kizlasova, M.A., Kishpanakov, V.A., Ovchinnikova, N.S., Tanzibaev, M.G., Yurin, Y.M., 1999. Atlas Respubliki Khakassiya (Atlas of the Republic of Khakassia – in Russian). Ministry of Government of the Republic of Khakassia.

Banks, D., 1998. The hydrogeochemistry of granitic groundwaters – illustrated by a comparison from Khakassia (Shira region), Norway (Oslo region) and the United Kingdom (Scilly Isles). In: Proc. of the 2nd Mezhdunarodnaya nauchnaya konferentsiya studentov i aspirantov i molodikh uchenikh im. akademika M.A. Usova, 'Problemi Geologii i Osvoeniya Nedr' (2nd International 'Academician M.A.Usov' Conference of Students, Aspirants and Young Scientists. Problems of Geology and the Exploitation of the Earth's Interior'). Tomsk Polytechnic University, 6–11 April, vol. 1. Tomsk Izd-vo NTL (Nauchno-Tekhnicheskoi Literaturi), Tomsk.

Banks, D., Parnachev, V.P., Berezovsky, A.Y., Garbe-Schönberg, D., 1998. The hydrochemistry of the Shira region, Republic of Khakassia, southern Siberia, Russian Federation – data report. Nor. Geol. Unders. Rep. 98.090.

Banks, D., Parnachev, V.P., Frengstad, B., Holden, W., Karnachuk, O.V., Vedernikov, A.A., 2001. The hydrogeochemistry of the Altaiskii, Askizskii, Beiskii, Bogradskii, Shirinskii, Tashtipskii & Ust' Abakanskii Regions, Republic of Khakassia, Southern Siberia, Russian Federation, data report. Nor. Geol. Unders. Rep. 2001.006.

Banks, D., Karnachuk, O.V., Parnachev, V.P., Holden, W., Frengstad, B., 2002a. Rural pit latrines as a source of groundwater contamination; examples from Siberia and Kosova. J. Chart. Instit. Water Environ. Manage. 16, 147–152.

Banks, D., Parnachev, V.P., Frengstad, B., Holden, W., Vedernikov, A.A., Karnachuk, O.V., 2002b. Alkaline mine drainage from metal sulphide and coal mines: examples from Svalbard and Siberia. In: Younger, P.L., Robins, N.S. (Eds.), Mine Water Hydrogeology and Geochemistry. Geol. Soc. Spec. Publ., vol. 198, pp. 287–296.

Gaevsky, N.A., Zotina, T.A., Gorbaneva, T.B., 2002. Vertical structure and photosynthetic activity of Lake Shira phytoplankton. Aquat. Ecol. 36, 165–178.

Harben, P.W., Kuzvart, M., 1996. Global geology – a: industrial minerals. Industrial Minerals Information, Metal Bulletin, London.

Hardie, L.A., Eugster, H.P., 1970. The evolution of closed-basin brines. Miner. Soc. Am. Spec. Publ. 3, 273–290.

Kalacheva, G.S., Gubanov, V.G., Gribovskaya, I.V., Gladchenko, I.A., Zinenko, G.K., Savitsky, S.V., 2002. Chemical analysis of Lake Shira water (1997–2000). Aquat. Ecol. 36, 123–141.

Kurlov, M.G., 1927. Kachinskaya steppe and its therapeutic wealth. Siberian archive of theoretical and clinical medicine (Tomsk) 2 (8–10), 852–856.

Kurlov, M.G., 1928. Classification of Siberian therapeutic mineral waters. Physiotherapeutic Institute, Tomsk.

Kurlov, M.G., 1929. Bibliographic guide on Siberian balneology. Physiotherapeutic Institute, Tomsk.

Luchitsky, I.V., 1960. Vulcanism and Devonian tectonics of the Minusinsk Basin. Akademija Nauk, Moscow (in Russian).

Makarenko, N.A., Petrov, A.I., Banks, D., Parnachev, V.P., 1999. Water resources, p. 18–43. In: Abdin, N.R., Bukatin, I.V., Dmitriev, V.E., et al. (Eds.), Krai taigi, ozer, pesher. Khakassia. Shirinskii raion (The land of taiga, lakes and caves. . .Khakassia. Shira region – in Russian), Khakassian University Press, Abakan.

Orlov, P.P., 1921. About the radioactivity of Siberian mineral waters. Proc. Inst. Siberian Invest. 3, 18–38 (Tomsk).

Parkhurst, D.L., 1995. User's guide to PHREEQC – a computer program for speciation, reaction-path, advective-transport, and inverse geochemical calculations. US Geol. Surv. Water-Resour. Invest. Rep. 95-4227.

Parnachev, V.P., Degermendzhy, A.G., 2002. Geographical, geological and hydrochemical distribution of saline lakes in Khakasia, southern Siberia. Aquat. Ecol. 36, 107–122.

Parnachev, V.P., Vasilev, B.D., Ivankin, G.A., et al., 1992. Geology and minerals of northern Khakassia. Izd-vo Tomsk State University (in Russian).

Parnachev, V.P., Balakhchin, V.L., Berezovsky, A.Y., Bukatin, I.V., Banks, D., Vidrina, S.M., Dmitriev, V.E., Kurbatsky, V.N., Larichev, V.E., Makarenko, N.A., Nekratov, N.A., Petrov, A.I., Prokofiev, S.M., Tanzibaev, M.G., 1997. Zhemchuzhina Khakassii: Prirodnii kompleks Shirinskovo raiona (Khakassian pearl: the natural system of the Shira region – in Russian). Khakas State University, Abakan. ISBN 5-7810-0052-6.

Parnachev, V.P., Vishnevezky, I.I., Makarenko, N.A., Petrov, A.I., Kopilova, Ju.G., Pokrovsky, D.S., Dutova, E.M., Turov, Ju.P., Klopotova, N.K., Djabarova, N.K., Banks, D., Berezovsky, A.Ja., 1999a. Vodnie resursi Shirinskovo raiona Respubliki Khakassia (Water resources of the Shira Region, Republic of Khakassia). Tomsk State University, Russia.

Parnachev, V.P., Banks, D., Berezovsky, A.Y., Garbe-Schönberg, D., 1999b. Hydrochemical evolution of Na–$SO_4$–Cl groundwaters in a cold, semi-arid region of southern Siberia. Hydrogeol. J. 7, 546–560.

Parnachev, V.P, Vishnevezky, I.I., Makarenko, N.A., Petrov, A.I., Kopilova, Yu.G., Smetanina, I.V., Karnachuk, O.V., Turov, Yu.P., Klopotova, N.G., Djabarova, N.K., Banks, D., Berezovsky, A.Ja., 2003. Prirodnie vodi Shirinskovo raiona, Respubliki Khakassia (Natural waters of the Shira Region, Republic of Khakassia – in Russian). Tomsk State University, Russia.

Plummer, L.N., Parkhurst, D.L., Fleming, G.W., Dunkle, S.A., 1988. A computer program incorporating Pitzer's equations for calculation of geochemical reactions in brines. US Geol. Surv. Water Resour. Invest. Rep. 88-4153.

Predtechensky, A.A., 1912. Health resorts of Siberia: Shira and Shunyet lakes. Sibirskaya lechebnaya gazeta 12, 144–147.

Savenkov, T.I., 1890. Materials to the medical and topographical description of the Shira lake (with map). Kudryavzev Press, Krasnoyarsk.

Stolbovoi, V., 1998. Soils of Russia: correlated with the revised legend of the FAO soil map of the world. International Institute for Applied Systems Analysis Interim Report IR-98-037. Laxenburg, Austria, p. 75.

Troëng, B., Riera-Kilibarda, C., 1996. Mapas temáticos de recursos minerales de Bolivia, Hoja Salinas de Garci Mendoza, Memoria Explicativa (Thematic maps of the mineral resources of Bolivia; Sheet Salinas de Garci Mendoza, Explanatory Memoir – in Spanish). Boletín del Servicio Geológico de Bolivia, No. 9.

US EPA, 1991. MINTEQA2/PRODEFA2, a geochemical assessment model for environmental systems: version 3.0 user's manual. US Environmental Protection Agency EPA/600/3-91/021, NTIS Accession No. PB91 182 469.